OUKA
Osaka University Knowledge Archive

Title	X-RAY DIFFRACTION STUDIES OF CHROMATOPHORE FROM PHOTOSYNTHETIC BACTERIUM, Rhodospirillum rubrum
Author(s)	片岡, 幹雄
Citation	大阪大学, 1980, 博士論文
Version Type	VoR
URL	https://hdl.handle.net/11094/742
rights	
Note	

Osaka University Knowledge Archive : OUKA

https://ir.library.osaka-u.ac.jp/

Osaka University

X-RAY DIFFRACTION STUDIES OF CHROMATOPHORE FROM PHOTOSYNTHETIC BACTERIUM, Rhodospirillum rubrum

by

Mikio KATAOKA

Department of Biophysical Engineering
Faculty of Engineering Science
Osaka University

June, 1980

PREFACE

Structural studies of photosynthetic apparatus is essential to understand the molecular mechanism of photosynthesis. Chromatophore, the photosynthetic apparatus of photosynthetic bacteria, exhibits all the partial reactions studied in chloroplast which is the photosynthetic apparatus of plant, except for the evolution of molecular oxygen, but is a much simpler system than chloroplast. Therefore, as was pointed out by Kamen (1963), the utilization of chromatophore is favorable for structural studies of photosynthetic apparatus. This thesis describes the X-ray diffraction studies of chromatophore isolated from *Rhodospirillum rubrum*, and reports obtained results about the structure of the photosynthetic unit.

This thesis consists of three chapters. Chapter I deals with the experimental studies: discovery of distinct X-ray diffraction pattern from chromatophore; X-ray and biochemical studies of isolated photoreaction unit. Chapter II deals with the theoretical background to interpret the X-ray diffraction pattern and discuss the structural features of the photosynthetic unit. The structure of chromatophore is depicted in Chapter III as a summary of the results obtained in Chapters I and II.

ACKNOWLEDGEMENTS

The author wishes to express his sincere appreciation to Professor Toshio Mitsui and Dr. Tatzuo Ueki for their many advices, valuable discussions, and encouragements during the course of this study. He also wishes to thank Professor Takekazu Horio (Institute for Protein Research, Osaka University) for his fruitful discussions, suggestions, and allowance of the use of the facilities in his laboratory throughout this study. He is greatly indebted to Dr. Jinpei Yamashita, Dr. Tomisaburo Kakuno, Dr. Gilbu Soe, Dr. Nozomu Nishi and Mr. Koichiro Tanaka (Institute for Protein Research, Osaka University), and Dr. Hideyuki Matsuda (College of Agriculture, Shimane University) for their technical assistances of preparations and biochemical procedures as well as for their helpful discussions, and to Dr. Keiichi Namba for his discussion on radial autocorrelation function. He is grateful to Dr. Shigehiro Morita and Dr. Tatsuo Miyazaki (Faculty of Science, University of Tokyo) for their discussions on Chapter I. Thanks are also due to all members in this Biophysics Laboratory and members in the Laboratory of Enzymology (Institute for Protein Research, Osaka University) for their helps offered during this study.

CONTENTS

ABSTRACT

Results obtained by the studies described in the thesis may be summarized as follows.

1. Chromatophore gives characteristic distinct X-ray diffraction pattern. The origin of the diffraction pattern is identified as the photosynthetic unit.
2. The photosynthetic unit is a molecular assembly having a diameter of 110 $\sim$ 130Å. The units are randomly distributed in chromatophore membrane.
3. The photosynthetic unit is composed of a main body and loosely bound components. The former is the photoreaction unit which contains the reaction center and light-harvesting bacteriochlorophyll protein complexes. The latter is the oxidation-reduction components such as ubiquinone-10 protein and cytochrome c_2.
4. The photosynthetic unit has as well-defined internal structure as to cause the distinct X-ray diffraction pattern. The structure has no translational symmetry, but may have a rotational symmetry.
5. Bacteriochlorophyll is an essential factor to maintain the characteristic structure of the photosynthetic unit.

INTRODUCTION

Photosynthesis is one of the most important and interesting vital phenomena. Biologically, it is indispensable: all organisms on the earth only except for chemoautotrophic organism require the products of photosynthesis, carbohydrates and molecular oxygen, for the energy source of their life; photosynthesis is one of the major elements to decide the evolution process. Geochemically, it is of consequence, too: accumulation of molecular oxygen to the atmosphere has been caused by photosynthesis. Human life is also considerably owing to it, especially as fossil fuel, not to speak of as food.

Phenomenologically, carbon dioxide, water, and light energy are the reactant, and oxygen and carbohydrates are the product in green plant photosynthesis. Pigment molecules, especially chlorophyll *a*, various enzymes and electron carriers, act in a catalytic manner in the reaction. Photosynthetic bacteria cannot use H_2O as the hydrogen donner and, therefore, cannot evolve molecular oxygen. Instead of H_2O, bacteria utilize organic compounds or inorganic sulfur compounds. Bacteria have bacteriochlorophyll as a major pigment instead of chlorophyll. van Niel (1935, 1941) proposed a general equation which describes both green plant and bacterial photosynthesis as:

$$CO_2 + 2H_2A \xrightarrow{h\nu} 2A + (CH_2O) + H_2O \qquad (1)$$

This equation generally expresses the phenomenon of photosynthesis.

However, this equation does not give the entire picture of photosynthesis. According to Kamen (1963), it can be defined as follows: Photosynthesis is a series of processes in which light energy is converted to chemical free energy that can be used for biosynthesis.

To consider a series of processes, Kamen (1963) has divided the various time scales into different eras (Fig. 1).

These series of processes take place efficiently and systematically in cellular photosynthetic apparatus.

The photosynthetic apparatus of plant and algae except for blue-green alga is called chloroplast, that of blue-green alga is "thylakoid", and that of bacteria is the intracellular membraneous structure. When the bacterial photosynthetic apparatus is isolated from the parent cell, it is called "chromatophore" (Pardee, Schachman & Stainer, 1952; Schachman, Pardee & Stainer, 1952). Chromatophore has a vesicular form with a diameter of about 600Å (*e. g.*, Oda & Horio, 1964). This is much smaller than chloroplast. For the sake of comparison, chloroplast and chromatophore are depicted in the same magnifying scale in Fig. 2. Chromatophores, like parent cell, exhibit all the partial reactions studied in chloroplast, except for the evolution

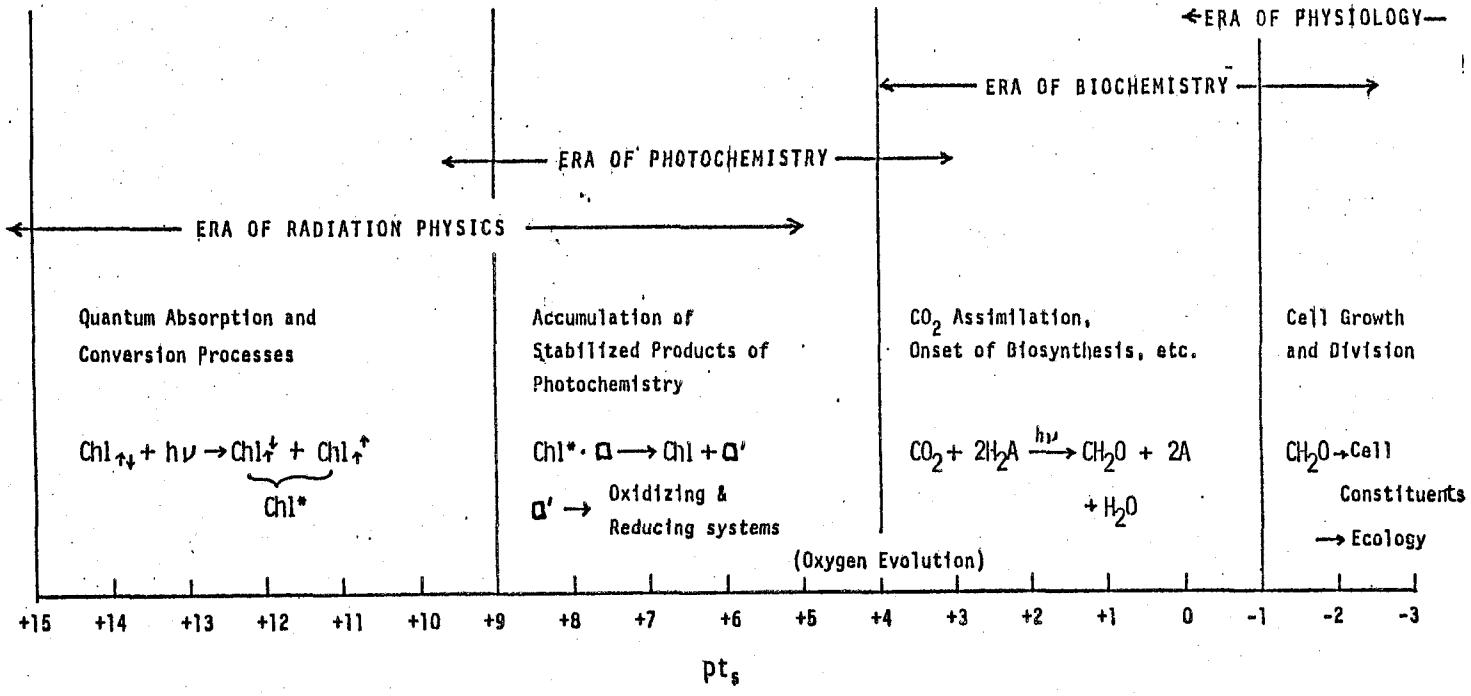

Fig. 1. The eras of photosynthesis (Kamen, 1963)
pt_s means logarithm of the reciprocal of time, expressed in seconds.
(pt_s 15 expresses 10^{-15} sec etc.)

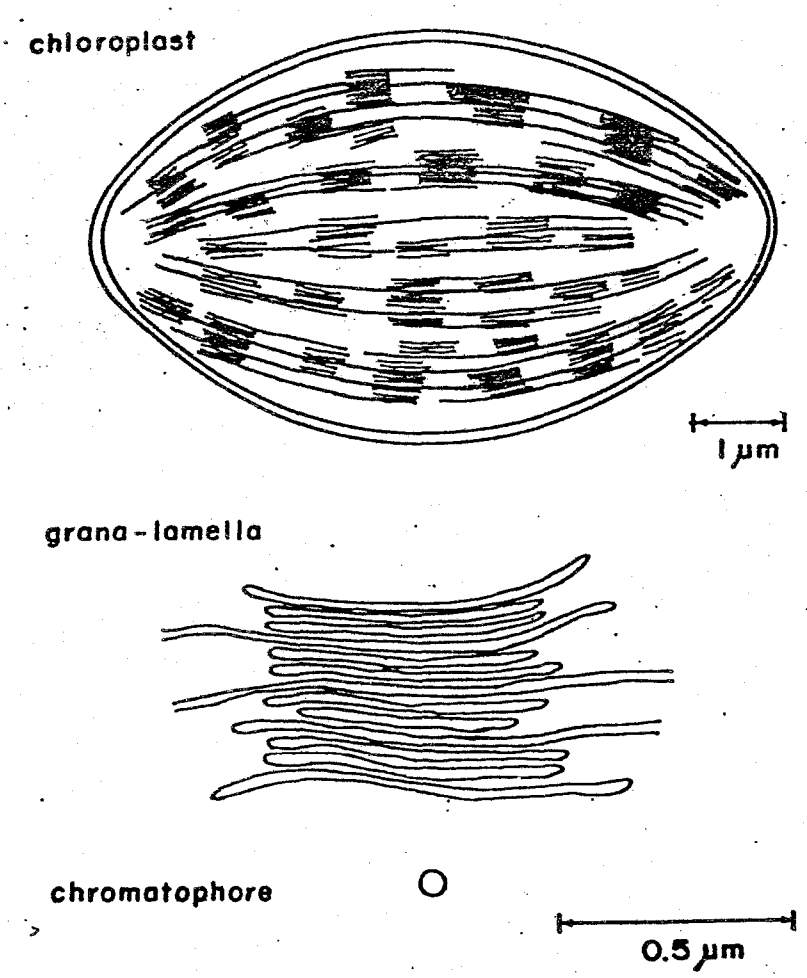

Fig. 2. Chloroplast and chromatophore.

of molecular oxygen.

Among the series of reactions of photosynthesis, primary processes, which are found in the first and second eras (Fig. 1), take place on the membrane of the photosynthetic apparatus. Chlorophyll or bacteriochlorophyll (abbreviated as Chl or BChl in the following) play an active role in the primary processes. When Chl or BChl bind with proteins in chloroplast or chromatophore, they exist in two different states of Chl (BChl), called light-harvesting Chl and reaction center Chl. The former is concerned with the light absorption and excitation energy transfer, and the latter with the charge separation. The quantum efficiency of the primary processes is strikingly high (nearly equal to 1) and this high efficiency is independent on temperature (Wright & Clayton, 1973; Parson, Clayton & Cogdell, 1975; Clayton & Yamamoto, 1976; also see Nishimura, 1975), suggesting the highly ordered structure of components. The assembly of Chl or BChl capable of primary processes is called the photosynthetic unit.

The concept of photosynthetic unit was firstly introduced by Emerson and Arnold (1932) with flash light experiment. They suggested that for every 2500 molecules of Chl, there exists one unit capable of evolving one molecule of oxygen. The concept of the photosynthetic unit was experimentally accepted (Thomas, Blaauw & Duysense, 1953; Kok, 1956; also see Huzisige, 1973; Govindjee &

Govindjee, 1975). The current concept of photosynthetic unit is depicted in Fig. 3. Each unit has about 300 molecules of light-harvesting Chl and a reaction center with electron transfer system. In fact, the units of chloroplast called photosystem I and photosystem II have been isolated to prove the existence of the photosynthetic unit (*e. g.*, Ogawa, Obata & Shibata, 1966; Huzisige, Usiyama, Kituti & Azi, 1969; Ohki & Takamiya, 1970). In the case of photosynthetic bacteria, Nishimura (1970) deduced that the photosynthetic unit contains 20 ∿ 40 BChl's. This bacterial photosynthetic unit, however, has not been isolated.

How are these units distributed in chloroplast or chromatophore? In what manner are Chl or BChl arranged in the unit? One of the essential ways to understand the mechanism of the primary processes of photosynthesis is the structural studies of the photosynthetic apparatus. Govindjee and Govindjee (1975) have pointed out the necessity of the structural studies as follows.

> "It appears that a highly ordered chloroplast membrane structure is necessary for the separation of positive and negative charges and their stabilization. The structure must somehow prevent the oxidizing and reducing equivalents from recombining to a significant extent, since recombination would result in the loss of energy as heat or light. Thus, a detailed study of the structure and composition of the chloroplast membrane is necessary for the understanding of the mechanisms of energy coupling."

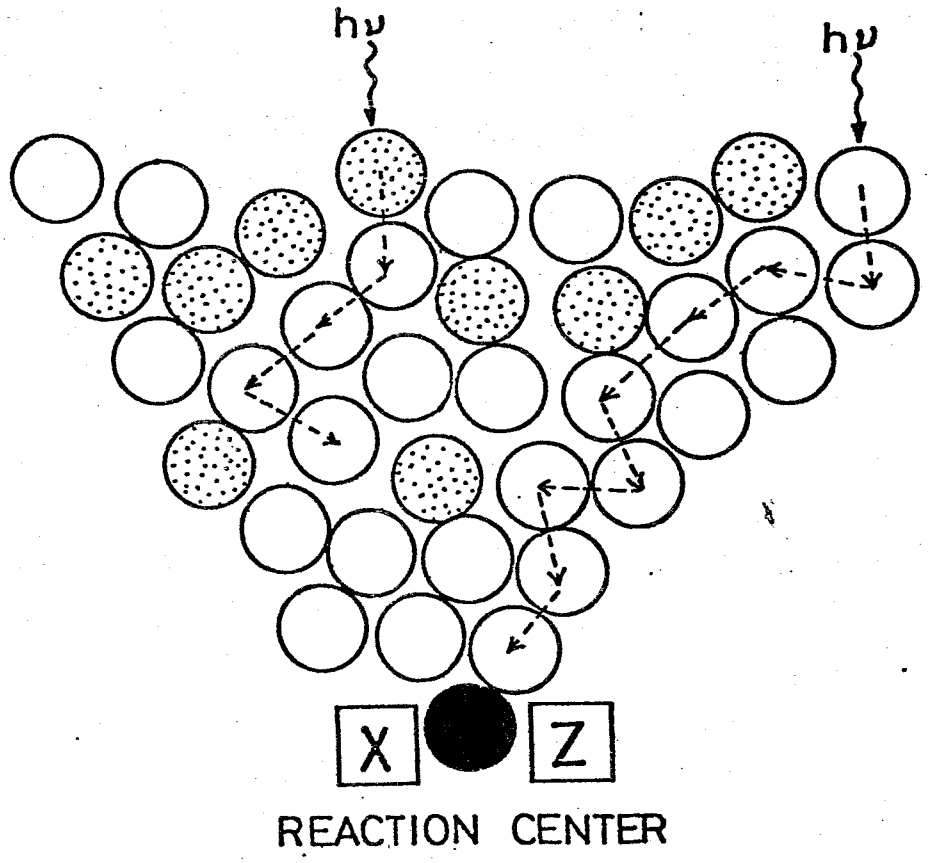

Fig. 3. Diagrammatic sketch of a photosynthetic unit.

○ : light-harvesting chlorophyll;

◎ : accessory pigment such as carotenoid;

● : reaction center chlorophyll;

X: primary electron donner; Y: primary electron acceptor;

----→: excitation energy migration.

The structure of chloroplast has been well investigated by electron microscopy (see Arntzen & Briantais, 1975; Tôyama, 1977). With the freeze-fracture method, two types of intramembrane particles were observed and related to photosystem I and II from circumstantial evidence (Staehelin, 1975, 1976; Miller, Miller & McIntyre, 1976). The fine structure within the particles, however, have not been investigated. The freeze-fracture electron microscope has not applied to the investigation of chromatophore, probably because its small size makes difficult to obtain the fracture face. X-ray diffraction studies of chloroplast have been carried out by Kreutz and Menke (Kreutz & Menke, 1960a, b, 1962; Menke, 1960; Kreutz, 1963a, b, 1964, 1965; Kreutz & Weber, 1966). They obtained both meridional and equatorial diffraction pattern up to the spacing 20Å. They intended to interprete the equatorial diffraction pattern on the basis of "quantasome" which was proposed by Park and coworkers (Park & Pon, 1961, 1963; Park & Biggins, 1964). However, it is doubtful of the existence of "quantasome" as both the structural and the functional units. Moreover, the origin of their diffraction pattern remained unknown. So far, we have no essential knowledge about the interactions between Chl or BChl in the photosynthetic apparatus.

The photosynthetic apparatus is one of the typical

biological membranes capable of energy transducing. Thus, the structure of the photosynthetic apparatus is also of interest from the viewpoint of the structure of biological membrane. In fact, the investigation of chloroplast structure led to the repeating unit theory for the structure of biological membrane (Benson, 1966).

The structure of biological membrane is widely believed in terms of the fluid-mosaic model by Singer and Nicolson (1972) (Fig. 4). Many observations seem to support the validity of the model. However, the model does not give knowledge on diverse and complicated functions of membranes, because it lacks information about interactions between functional components in membranes. In order to promote a better understanding in function-structure relationship, it is necessary to clarify molecular components of the membrane and their mutual arrangement.

X-ray diffraction technique is a powerful approach to elucidate the structure of membrane, as well as electron microscopy. Structural studies of the purple membranes of *Halobacterium halobium* by diffraction techniques (Blaurock & Stoeckenius, 1971; Henderson, 1975; Blaurock, 1975; Unwin & Henderson, 1975) have promoted the structural studies of biological membrane, especially of membrane proteins, and have raised the question of whether the in-plane structural order is an exceptional feature of very limited biomembranes or whether it is somewhat more

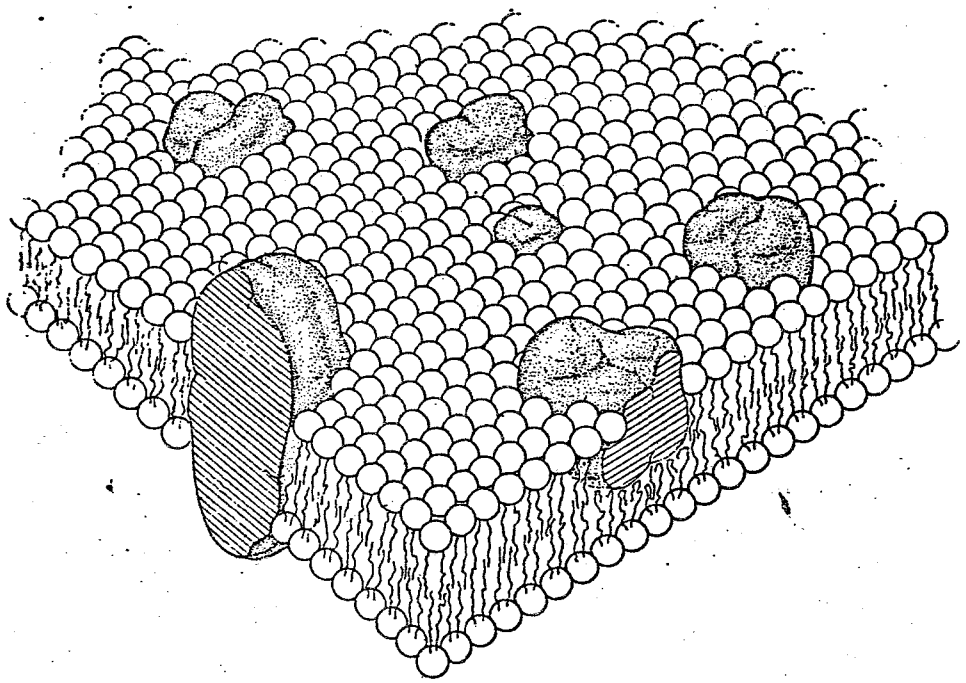

Fig. 4. The fluid-mosaic model of the structure of biological membrane (Singer & Nicolson, 1972).

common. By X-ray diffraction, we have partly answered this problem that the structural order exists in the chromatophores of *Rhodospirillum rubrum* and *Rhodopseudomonas sphaeroides* and the outer membranes of *Salmonella typhimurium* and *Escherichia coli* (Ueki, Kataoka & Mitsui, 1976; Ueki, Mitsui & Nikaido, 1979). Several workers have also reported the regular structure existing in the membrane (Dupont, Cohen & Changeux, 1974; Mannella & Bonner, 1975; Casper, Goodenough, Makowski & Phillips, 1977). In spite of these observations, it seems that any intensive structural studies of biological membranes have not intended except for the purple membrane.

There are two problems which we encounter in X-ray diffraction studies of biomembranes, as below.

(1) Identification of the X-ray scatterer: biomembranes consist of many molecular species with a few exceptions such as the purple membrane. Therefore, it is of great importance to identify which molecules give rise to X-ray diffraction patterns. Some approaches are available to this problem.

(1-i) Use of mutant: when we can obtain some mutants which lack specific components, they lead to the identification of the scatterer. With this method, the X-ray scatterer of the outer membrane of *S. typhimurium* revealed to be porins (Ueki *et al.*, 1979).

(1-ii) Solubilization: when we can find a good condition,

the X-ray scatterer will be solubilized from the membrane. By this method, we have identify the X-ray scatterer of chloroplast as photosystem I (Tsukamoto, 1980; Tsukamoto, Ueki, Kataoka & Mitsui, 1980).

(1-iii) Reconstitution: it is also effective to reconstruct the X-ray scatterer from the solubilized components. By this method, the X-ray scatterer of the outer membrane has been identified as the porin trimer (Ueki, Tanaka, Nakae & Nikaido, 1980).

(1-iv) Modification or digestion: the modification or the digestion by biochemical treatment lead to reveal the features of the X-ray scatterer.

(2) Structure of the X-ray scatterer: this is, so called, X-ray structure analysis. However, different from the case of crystal structure analysis, few analytical methods have been developed. In this purpose, radial autocorrelation function was strictly examined (Kataoka & Ueki, 1980).

In the thesis, the author reports the intensive structural studies of chromatophore membrane isolated from a photosynthetic bacterium, *Rhodospirillum rubrum* (Fig. 5), in conjunction with its function. He refers to both of the problems mentioned above. In Chapter I, the identification of the X-ray scatterer is mainly described. The techniques of the solubilization and the reconstitution are applied to reveal the scatterer. The relation between the X-ray scatterer and the photosynthetic unit is also discussed.

Chapter II deals with the interpretation of the X-ray diffraction pattern. The approach by the radial auto-correlation function is strictly developed. The structural features of the scatterer are discussed on the basis of the function.

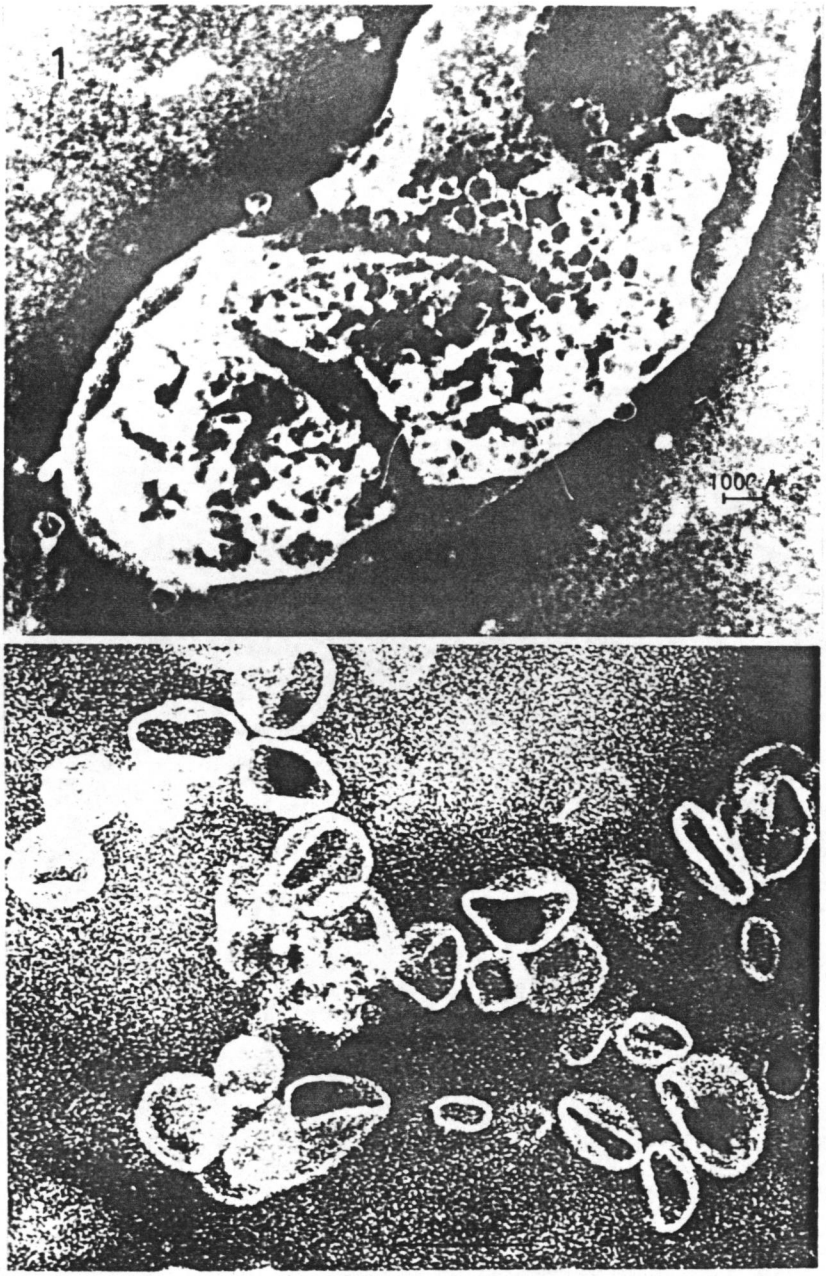

Fig. 5. Electron micrographs of (1) *Rhodospirillum rubrum* and (2) chromatophores isolated from the cell. (Oda & Horio, 1964)

CHAPTER I

X-RAY DIFFRACTION STUDIES OF CHROMATOPHORE, SOLUBILIZED FRACTIONS AND RECONSTITUTED SYSTEMS

I-1. INTRODUCTION

The structure of chromatophore, the photosynthetic apparatus of photosynthetic bacteria, has been investigated by several workers. By electron microscopy, some have observed the particulated fine structure on the chromatophore membrane from *Rhodospirillum rubrum* (Holt & Marr, 1965; Oelze & Golecki, 1975), *Rhodopseudomonas sphaeroides* (Lommen & Takemoto, 1978) and *Rhodopseudomonas viridis* (Giesbrecht & Drews, 1966; Miller, 1979). On the other hand, Oda and Horio (1964) have observed smooth surface without any fine structure in the case of *R. rubrum* chromatophore. It seems that these observations give no essential knowledges about function-structure relationship of chromatophore. The X-ray diffraction studies of chromatophore from *Rps. sphaeroides* were previously reported by Langridge, Barron and Sistrom (1964) and Pape, Menke, Weick and Hosemann (1974). Both were mainly concerned with the diffraction patterns in the direction perpendicular to the membrane plane and discussed the electron density profile projected onto the membrane normal. They, however, obtained rather poor diffraction patterns corresponding to the in-plane structure and hence did not refer to it.

We have found that chromatophore membranes of *R. rubrum* and *Rps. sphaeroides* give distinct X-ray diffraction patterns which arise from protein assemblies in chromato-

phore (Ueki *et al.*, 1976). Such a diffraction pattern indicated that the X-ray scatterer, *i. e.*, the protein assembly has a fairly rigid structure in the membrane and is expected to be isolated under mild conditions. There have been several complexes isolated by detergents: light-harvesting bacteriochlorophyll protein complexes (Feick & Drews, 1978; Moskalenko & Erokhin, 1978; Cuendet, Zürrer, Snozzi & Zuber, 1978) and reaction center complexes (Reed, Raveed & Israel, 1970; Clayton & Haselkorn, 1972; Noël, Rest & Gingras, 1973; Okamura, Steiner & Feher, 1974). Recently, we have also succeeded to isolate the photoreaction unit which consists of light-harvesting bacteriochlorophyll proteins and reaction centers (Nishi, Kataoka, Soe, Kakuno, Ueki, Yamashita & Horio, 1979). X-ray diffraction studies were performed on chromatophore and isolated protein complexes to identify the X-ray scatterer in chromatophore from *R. rubrum*.

One of the most important purposes of structural studies of chromatophore is to understand the interaction between bacteriochlorophyll molecules. Bacteriochlorophyll is one of the major components of chromatophore (Kakuno, Bartsch, Nishikawa & Horio, 1971; Shioi, Takamiya & Nishimura, 1974), and plays an essential role in the primary process of photosynthesis. The high efficiency of energy transfer between bacteriochlorophyll molecules implies the strong interactions between them. The role of bacterio-

chlorophyll in constructing the X-ray scatterer was examined by treatment of chromatophore with acetone or chlorophyllase.

I-2. EXPERIMENTAL PROCEDURES

(a) Cell Culture and Preparation of Chromatophore.

The carotenoid-less blue-green mutant of *Rhodospirillum rubrum*, strain G-9, was used throughout this study. Cells were cultured anaerobically in the light (Horio, Nishikawa, Katsumata & Yamashita, 1965).

The grown cells were collected and washed with 0.1 M Tris-HCl buffer (pH 8.0), 0.1 M Tris-HCl buffer containing 0.01 M ethylenediaminetetraacetate (EDTA) (pH 8.0), 0.1 M Tris-HCl buffer containing 0.5 M potassium tartrate (pH 8.0) and then with 0.01 M Tris-HCl buffer (pH 8.0). The washed cells were suspended in 0.1 M Tris-HCl buffer (pH 8.0), and disrupted by sonication (10kHz by Sonifier model 350, Branson Sonic Power Co.) at 0 ∿ 10°C for 12 min. (Nishi *et al.*, 1979). The suspension obtained was centrifuged at 8,000 × *g* for 10 min to remove unbroken cells. The supernatant was centrifuged at 30,000 × *g* for 30 min. The resulting supernatant was centrifuged at 105,000 × *g* for 90 min. The precipitate, crude chromatophore, was collected and were centrifugally washed three times with

0.1 M Tris-HCl buffer (pH 8.0). The chromatophores finally obtained were suspended in 0.1 M Tris-HCl buffer (pH 8.0) so that A_{873nm} of the suspension was approximately 200 (Horio *et al.*, 1965).

(b) Solubilization of Chromatophore with Mixture of Cholate and Deoxycholate.

A chromatophore suspension (A_{873nm}=200) was diluted with an equal volume of 0.1 M Tris-HCl buffer containing 2% cholate and 4% deoxycholate (pH 8.0), stirred overnight, and sonicated at 10 kHz for 3 min. The sonicated suspension was centrifuged for 1 h at 100,000 × *g*. The resulting supernatant was collected. The precipitate was resuspended in 0.1 M Tris-HCl buffer containing 1% cholate and 2% deoxycholate (pH 8.0), sonicated at 10 kHz for 3 min, and centrifuged for 1 h at 100,000 × *g*. The resulting supernatant was combined with the first supernatant, and subjected to ammonium sulfate fractionation. The precipitate in 30%-saturated ammonium sulfate solution was collected, suspended in 0.05 M Tris-HCl buffer containing 0.1% cholate and 0.3% deoxycholate (pH 8.0), and dialyzed against the buffer containing the detergents. The dialyzed solution was designated as cholate-deoxycholate soluble fraction (C-DOC soluble fraction). All the procedures described above were carried out at 4°C and in the dark as far as possible (Nishi *et al.*, 1979). The

C-DOC soluble fractions were subjected to molecular-sieve chromatography on a Sepharose 6B column. Four fractions were finally obtained (named F1, F2, F3 and F4 in the order of elution profile in terms of A_{280nm}) (see Fig. I-3). F1 and F2 were purified with three successive molecular-sieve chromatography on a Sepharose 6B column. F3 and F4 were similarly purified on an Ultrogel AcA22 column and a Sephadex G-75 column, respectively (Nishi *et al.*, 1979). An aliquot of F2 was also used for X-ray experiment without purification (called crude F2 below).

(c) Reconstitution of the X-ray Scatterer.

Cytochrome c_2 which was purified from cells grown in the light (Horio & Kamen, 1961) and ubiquinone-10 protein which was purified from F4 (Nishi *et al.*, 1979) were kindly supplied by Dr. N. Nishi (Institute for Protein Research, Osaka University). Total polar lipids which were extracted from chromatophore by acetone-methanol solution were gifts from Dr. H. Matsuda (College of Agriculture, Shimane University).

Purified F2, ubiquinone-10 protein, cytochrome c_2 and ethanol solution of total polar lipids were added gently in 0.05 M Tris-HCl buffer (pH 8.0) in this order so that final bacteriochlorophyll concentration was A_{865nm}=2, and their molar ratios became 1, 5, 5 and 3800 (Matsuda, Kakuno & Horio, 1980). In some cases, ubiquinone-10 protein and

cytochrome c_2 or polar lipids were not mixed. The procedures were performed under dark condition at 20°C.

(d) Treatment of Chromatophore with Acetone.

Chromatophore was treated with various ratios of acetone/water as follows. 2 ml of chromatophore suspension (A_{873nm}=100) was diluted with an appropriate volume of acetone and 0.1 M Tris-HCl buffer (pH 8.0) to make the total volume 10 ml, then stirred well for 30 ∿ 60 sec. The solution was centrifuged at 6,000 × g for 15 min. The solution of 30% or lower concentration of acetone were centrifuged at 105,000 × g for 90 min. An aliquot of supernatant was used for analysis of removed bacteriochlorophyll. The precipitate was suspended in 0.1 M Tris-HCl buffer (pH 8.0), washed centrifugally, and was used for X-ray experiment.

(e) Treatment of Chromatophore with Chlorophyllase.

Chlorophyllase which was extracted and purified from greened rye seedlings (Tanaka, 1980) was a gift from Mr. K. Tanaka (Institute for Protein Research, Osaka University).

Chromatophores were treated with the enzyme as follows (Tanaka, 1980). The reaction mixture comprised chromatophores (A_{873nm}=1.5), an appropriate volume of acetone, 1.0 ml of chlorophyllase solution, 20 µl of 0.1 M ascorbate, 0.2 ml of 0.2 M phosphate buffer (pH 6.5) and water to

make the total volume 2.0 ml. The pH of the reaction mixture was adjusted to 7.5 with NaOH or HCl. The reaction was carried out at 30°C in a stoppered tube and in the dark.

(f) Optical Spectroscopy.

Absorbances were measured at 25°C with a Cary model 17 spectrophotometer or a Shimadzu double beam spectrophotometer UV-200. Light-induced absorbance change was measured at 25°C with a Union High-Sense spectrophotometer with actinic light, 590 nm.

(g) Biochemical Procedures.

Bacteriochlorophyll extracted by acetone was estimated from the absorbance in diethylether as follows. Diethylether (2 ml) and 6 ml of KCl-saturated water were added to 2 ml of the extraction of chromatophore by acetone. The mixture was vigorously blended to complete extraction of pigment, and then centrifuged at 8,000 × *g* for 15 min. The absorbance of the resultant upper layer (ether layer) was measured at 773 nm (ε_{mM}=91.1 $cm^2 \cdot mM^{-1}$) (Smith & Benitez, 1955).

Sodium dodecylsulfate (SDS)-polyacrylamide concentration-gradient slab gel electrophoresis was carried out according to the method of Laemmli (1970). All the procedures were described previously (Nishi *et al.*, 1979).

(h) Preparation of Specimen for X-ray Diffraction Experiment.

Two kinds of specimens were used for X-ray studies: wet pellets and dried specimens.

Pellets of chromatophores were prepared by centrifugation at 105,000 × *g* for 90 min. Solubilized fractions, F1, F2 and F3, were centrifuged at 150,000 × *g* for more than 5 h and the resultant pellets were collected. Each reconstituted system was centrifuged at 105,000 × *g* for 90 min to obtain the pellets. Chromatophores treated with acetone or chlorophyllase were also pelleted by centrifugation. Each pellet was sealed into a thin-walled glass capillary (10 μm in the wall thickness and 1.0 mm or 1.5 mm in the diameter). Solubilized fraction, F4, was not pelleted, and hence the suspension was sealed into a glass capillary and used for the X-ray experiment.

The dried sample of chromatophore was prepared by placing the pellet on a clean slide glass. They were dried in a refrigerator for more than 2 days. A thin strip, cut off from the dried matter, was also sealed into a glass capillary.

(i) X-ray Diffraction Experiment.

The source of X-ray was a fine-focus rotating-anode X-ray generator made by Rigaku Denki (modified RU-100 unit) operated at 40 kV with tube current 30 mA giving Cu-Kα radiation (λ=1.542Å). An effective focal spot was 100 ×

100 μm^2 at grancing angle 6°. An Elliott type toroid optics (Elliott, 1965) with a series of double sector appertures (distributed by Marconi Elliott Avionic System Ltd.) was used in a small-angle diffraction camera *in vacuo*. The diffraction pattern was recorded either on Fuji medical KX film, Sakura cosmic ray film or on Kodak medical NS-54T film. Specimens were placed at 50 ∿ 100 mm from the films and the distance was calibrated by powder diffraction pattern of sodium myristate. The X-ray path between the source and the film was evacuated to eliminate air scattering. The temperature of specimens was maintained below 4°C during exposure by circulating chilled water through the specimen holder. The exposure time was usually 15 ∿ 50 h for Fuji films and 3 ∿ 5 h for Sakura or Kodak films. The photographic density (optical density) was measured with a Nalumi C-type microdensitometer and was converted to intensity data by using a calibrated intensity scale.

I-3. RESULTS

(a) X-ray Diffraction Pattern of Chromatophore.

The wet pellet of chromatophore gave diffraction pattern consisting of a series of distinct diffraction rings in the region of moderate scattering angle (spacing

d of 6Å < d < 22Å), and occasionally a sharp ring at d = 4.2Å, as shown in Fig. I-1 (a).

A sharp 4.2Å reflection indicates crystalline packing of hydrocarbon chains of lipids in the membranes. In some cases, this ring could not be observed but broad ring at d = 4.6Å. Broad 4.6Å reflection indicates that the packing of hydrocarbon chains are in liquid phase. These reflections suggests that the region occupied by lipids is fairly extended in the chromatophore membrane as the fluid-mosaic model.

The dried specimens gave diffraction pattern as shown in Fig. I-1 (b), when the incident beam was parallel to the plane attached to the slide glass. We have termed the direction parallel to this plane equator and the perpendicular direction meridian. As is clear from Fig. I-1 (b), the dried specimen is oriented. The 4.2Å reflection came out as an equatorial reflection, proving that the membranes lie approximately parallel to the surface of slide glass (Ueki *et al.*, 1976). (In Fig. I-1 (b), the film-to-specimen distance was too long to obtain 4.2Å reflection.) Therefore, equatorial reflections correspond to the in-plane structure of a membrane.

The moderate-angle diffraction pattern appeared in the equatorial direction, as is clear from Fig. I-1 (b). This fact indicated that there exists a highly organized in-plane structure in the chromatophore membrane.

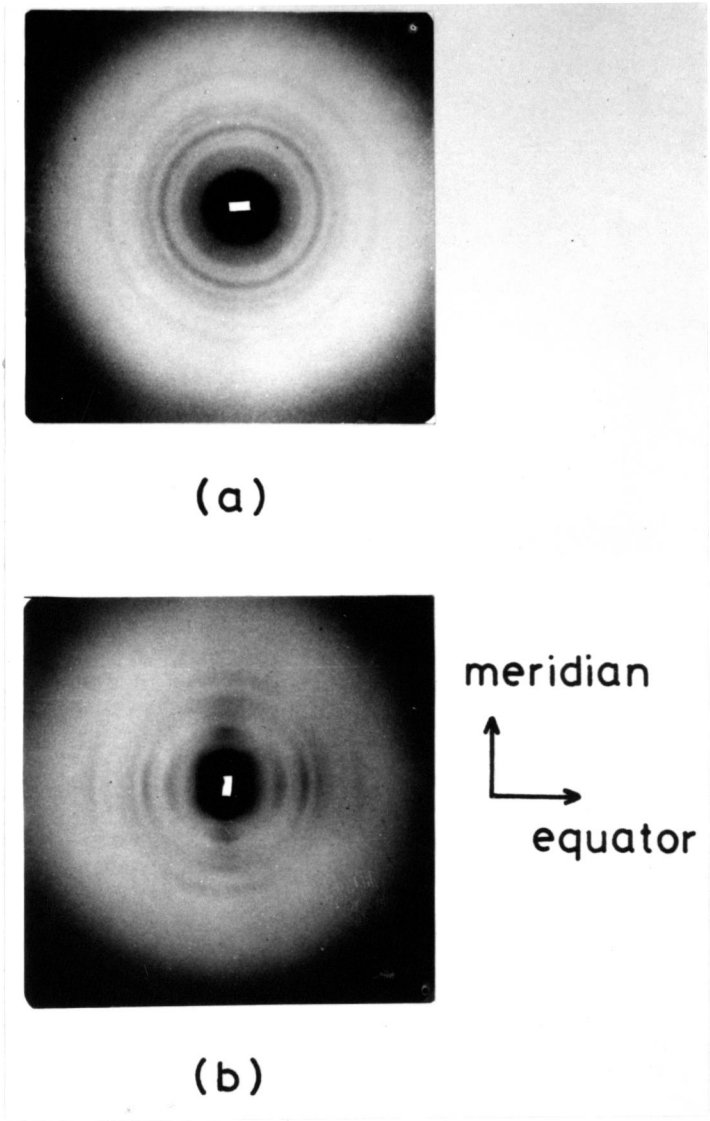

Fig. I-1. X-ray diffraction photographs of chromatophore.
(a) wet pellet (unoriented specimen),
(b) dried sample (oriented specimen).
See text for equator and meridian.

Figure I-2 shows densitometer traces of the diffraction pattern of an unoriented specimen and the equatorial diffraction of an oriented specimen. The moderate-angle equatorial reflection have a one-to-one correspondence with those of an unoriented specimen. Although dried specimens have higher signal-to-noise ratio than wet specimens, there were no appreciable differences between their spacings and intensities, and hence, the structure (X-ray scatterer) was well preserved upon drying process.

In addition to the equatorial reflection, an off-meridional reflection was observed at $d \simeq 37$Å in the dried specimen, suggesting that the protein molecules are not in a plannar arrangement.

(b) X-ray Diffraction Patterns of Solubilized Fractions.

Figure I-3 shows the elute pattern obtained by molecular-sieve chromatography of the C-DOC soluble fraction on a Sepharose 6B column. The elution profile in terms of A_{280nm} showed two sharp peaks at fraction number 19 and 32, a shoulder around fraction number 40 and a broad peak at numbers 52 $\sim$ 60. These fractions were gathered independently and designated F1, F2, F3 and F4 in the order of elution. Most of bacteriochlorophyll (A_{873nm}) solubilized from chromatophores appeared in F1 and F2. The F4 contains no bacteriochlorophylls. The F3 shows considerably high ratio of $(-\Delta A_{865nm}/A_{873nm})$ (reaction

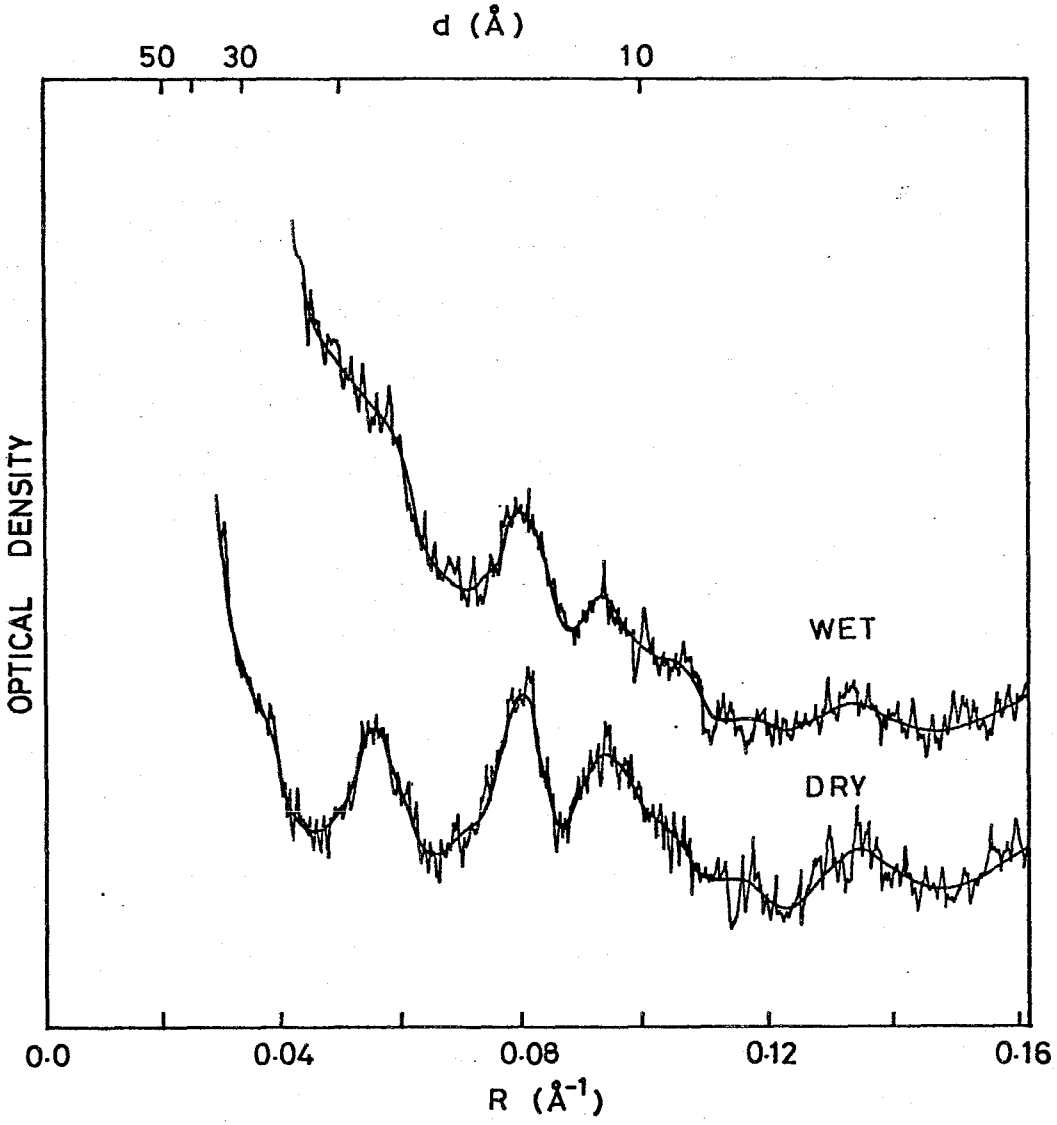

Fig. I-2. Densitometer traces of diffraction pattern from wet specimen of chromatophore (unoriented sample) and equatorial diffraction pattern from dried specimen (oriented sample), shown in Fig. I-1. A shoulder at $R \simeq 0.035 \mathring{A}^{-1}$ is due to contamination of meridional reflection.

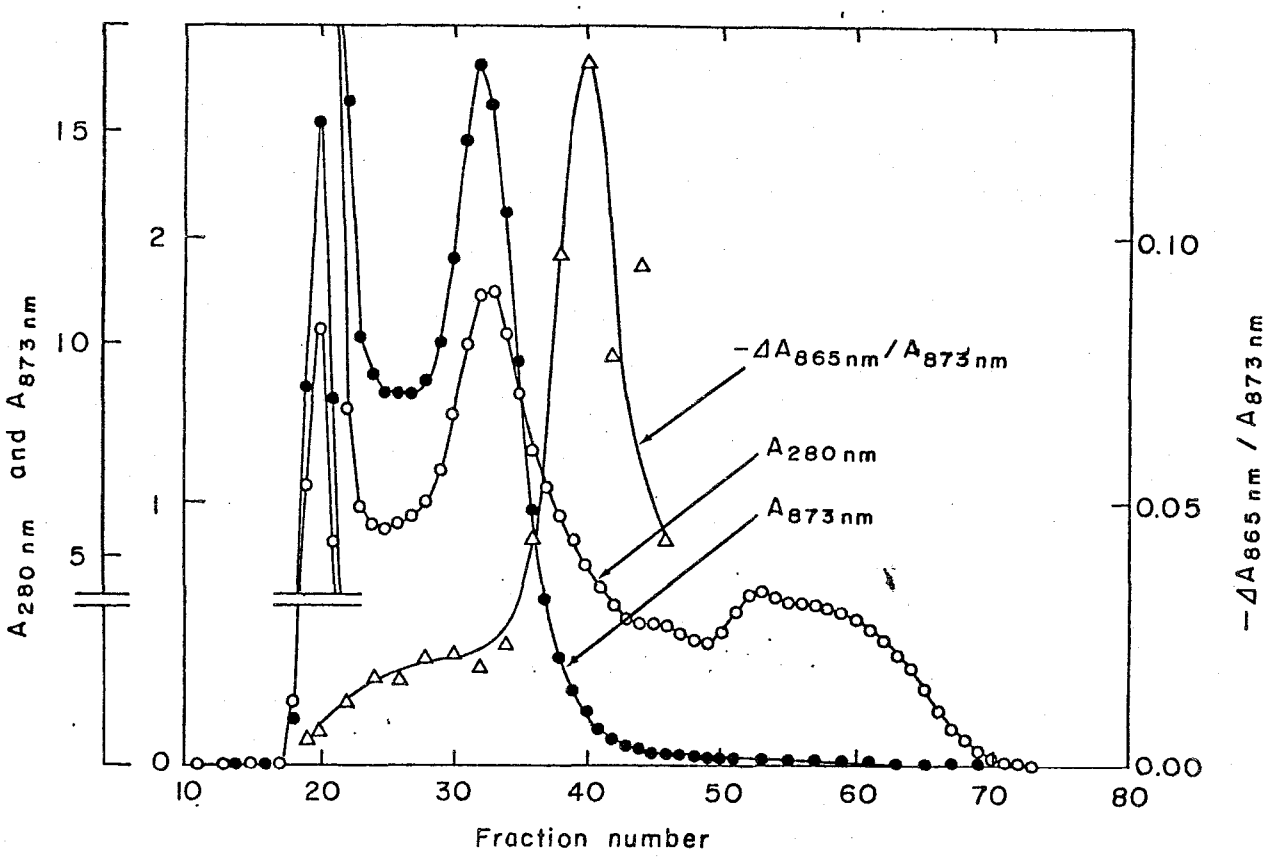

Fig. I-3. Molecular-sieve chromatography of C-DOC soluble fraction on Sepharose 6B column. The C-DOC soluble fraction (A_{873nm}=60) (30 ml) was charged on a Sepharose 6B column (5 × 90 cm) and eluted with 0.05 M Tris-HCl buffer containing 0.1% cholate and 0.3% deoxycholate (pH 8.0), collecting 25-ml fractions. Other experimental conditions are described in the text.

center activity/bacteriochlorophyll concentration). The ratios are approximately 0.007, 0.02 and 0.13 at the peaks of F1, F2 and F3, respectively. The fractions F1, F3 and F4 were identified as conjugated forms of F2, reaction center and ubiquinone-10 protein, respectively (Nishi *et al.*, 1979).

X-ray diffraction patterns of these fractions are shown in Fig. I-4. The moderate-angle diffraction pattern due to the in-plane structure of chromatophore was still observed for F1 and F2 but disappeared for F3 and F4. F1 and F2 gave essentially the same diffraction patterns each other, as shown in Figs. I-4 (a) and (b). This fact supported the result that F1 is conjugated forms of F2 (Nishi *et al.*, 1979). The diffraction pattern of F2 quite resembles to that of chromatophore, as shown in Figs. I-1 and I-4 (b).

Comparison of moderate-angle diffraction profiles of chromatophore, crude F2 and purified F2 are shown in Fig. I-5 (see EXPERIMENTAL PROCEDURES for crude and purified F2). In these profiles, we can find two minor differences: decreases of intensities of diffraction maxima at $d \simeq 18\mathring{A}$ and $10.5\mathring{A}$ (indicated by arrows in Fig. I-5). The relative intensities of these reflections decreased as the purification proceeded, but the positions of peaks did not shift appreciably. These changes, thus, strongly implied that some components are removed from the X-ray

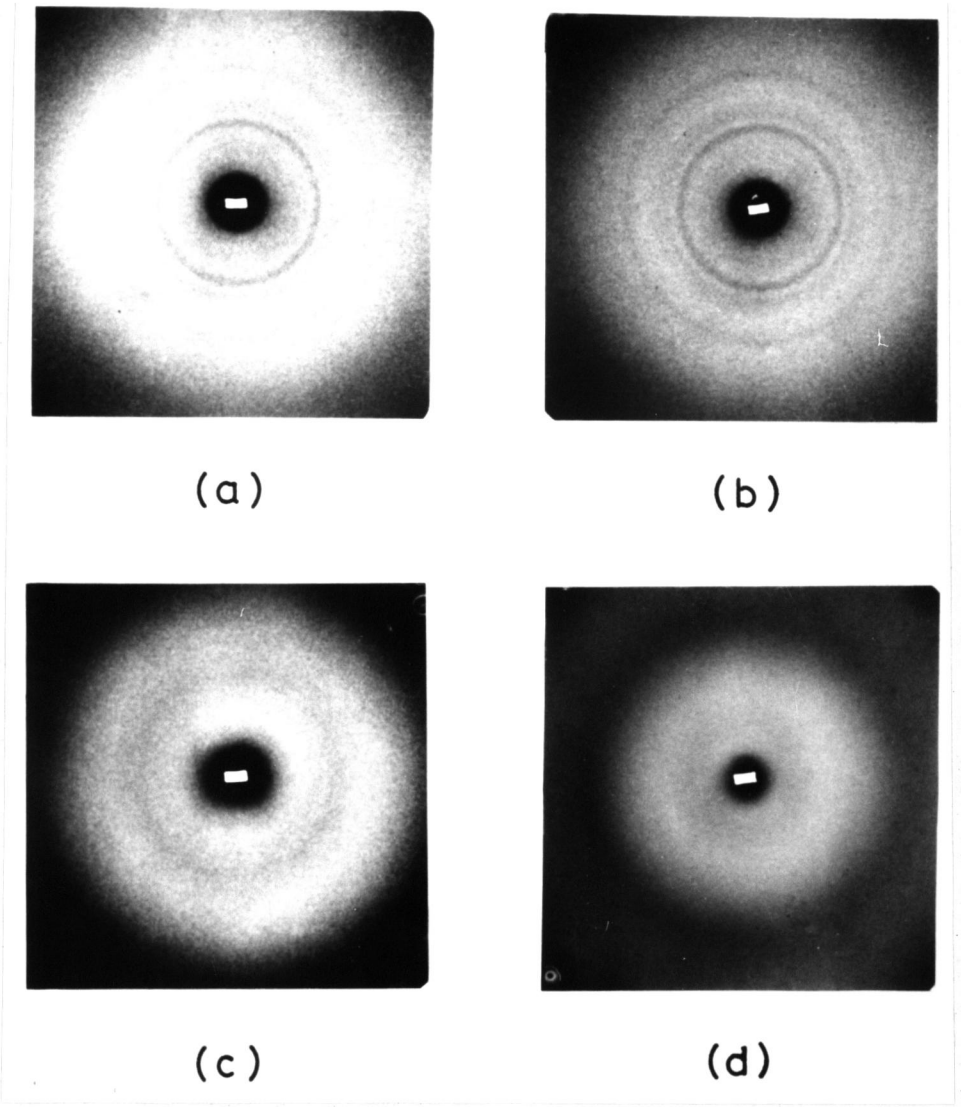

Fig. I-4. X-ray diffraction photographs of solubilized fractions. (a) F1, (b) F2, (c) F3 and (d) F4. All photographs were taken under the same experimental conditions.

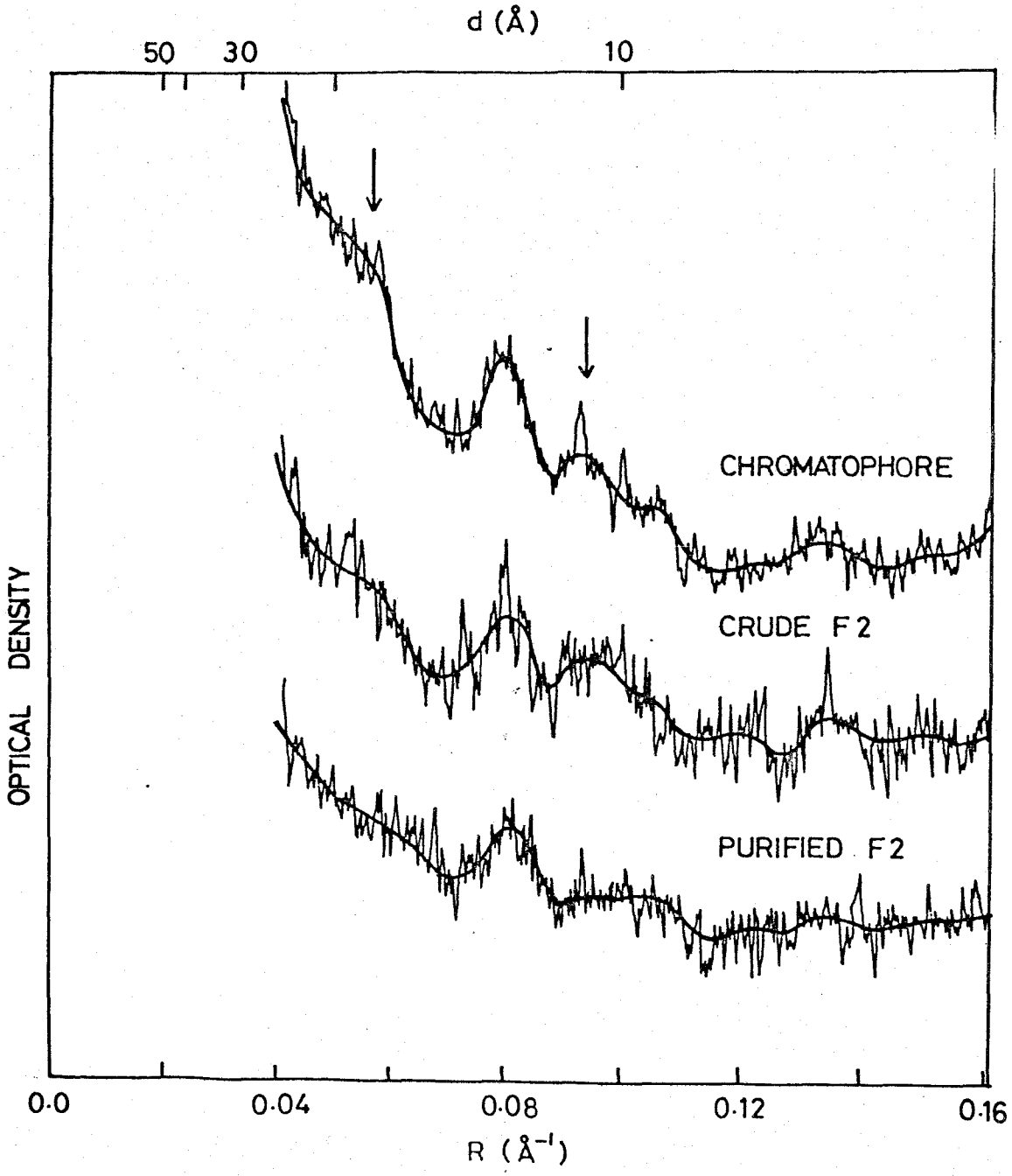

Fig. I-5. Densitometer traces of X-ray photographs from chromatophore, crude F2, and purified F2.
Two arrows indicate diffraction maxima at $d \simeq 18$Å and 10.5Å, respectively.

scatterer in the process of the isolation and purification. In spite of these differences, good resemblance in these diffraction profiles to each other led to a conclusion that F2 is the basic structure of the X-ray scatterer existing in chromatophore.

There were no distinct diffraction patterns except for diffuse halo at $d \simeq 10\text{Å}$ in Fig. I-4 (c). The diffuse halo is a characteristic feature of α-protein (Arndt & Riley, 1952). F4 gave diffuse halos at $d \simeq 16.7\text{Å}$ and 6.3Å as shown in Fig. I-4 (d). The structural parameters of α-helix do not contain these values, and the value 6.3Å is close to the dimension of repetition of unit in β-sheet. However, diffraction pattern of F4 remained uninterpreted in detail. It was, from these patterns, concluded that there are no regular arrangement in F3 and F4.

(c) Characterization of F2.

The purified F2 was nearly homogeneous with respect to the concentration ratio of bacteriochlorophyll to protein in the last chromatography, and had an apparent particle weight of 7×10^5 daltons (Fig. I-6). Its absorbance spectrum was similar to that of chromatophores, except that the main peak due to bacteriochlorophyll was at 865 nm, which is 8 nm shorter than with chromatophores (Fig. I-7). The purified F2 contained 33 molecules of bacteriochlorophyll,

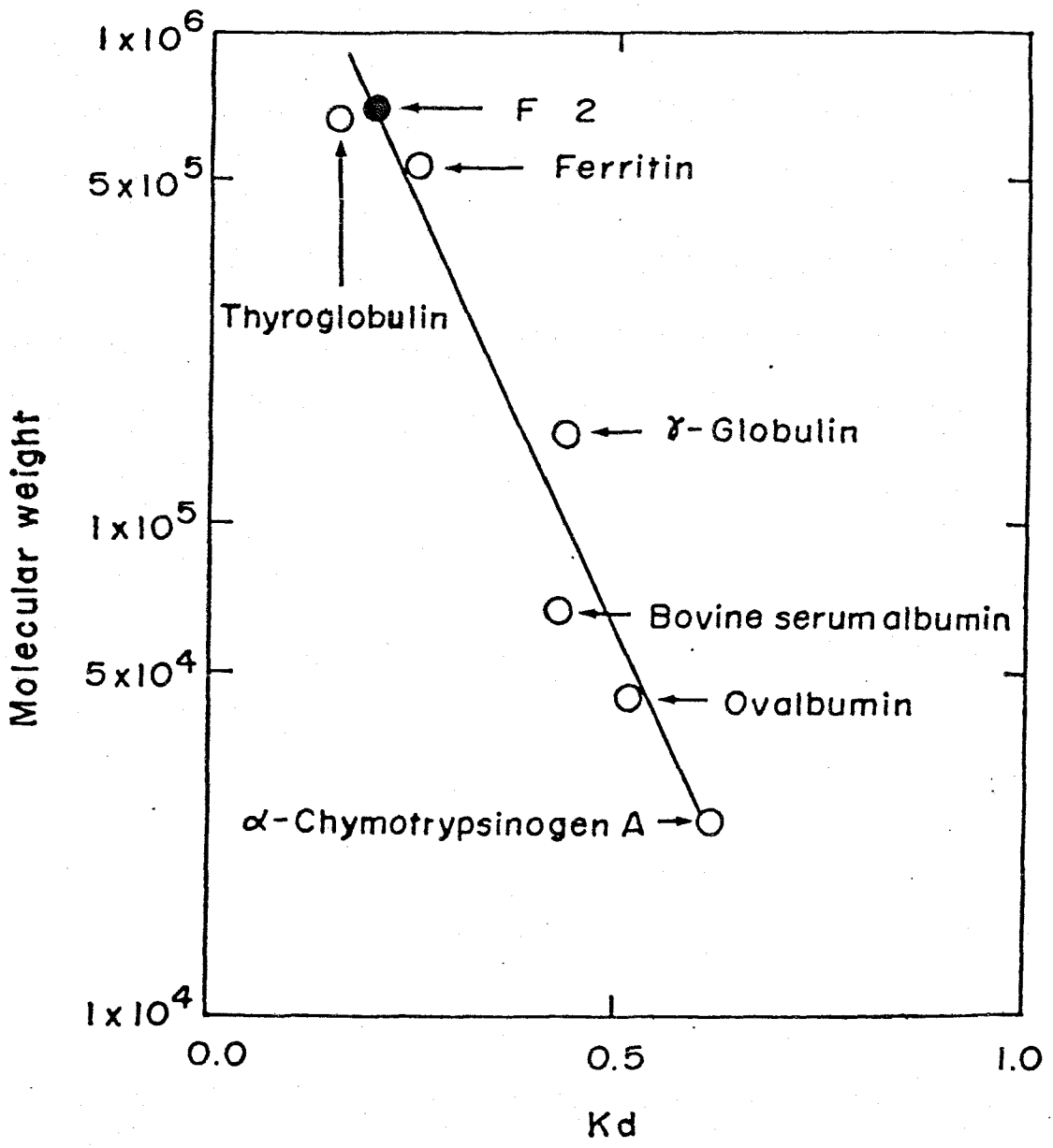

Fig. I-6. Estimation of particle weight of purified F2 by molecular-sieve chromatography on Sepharose 6B column. The experimental conditions were the same as for Fig. I-3, except for the use of various molecular weight markers. (Nishi *et al.*, 1979)

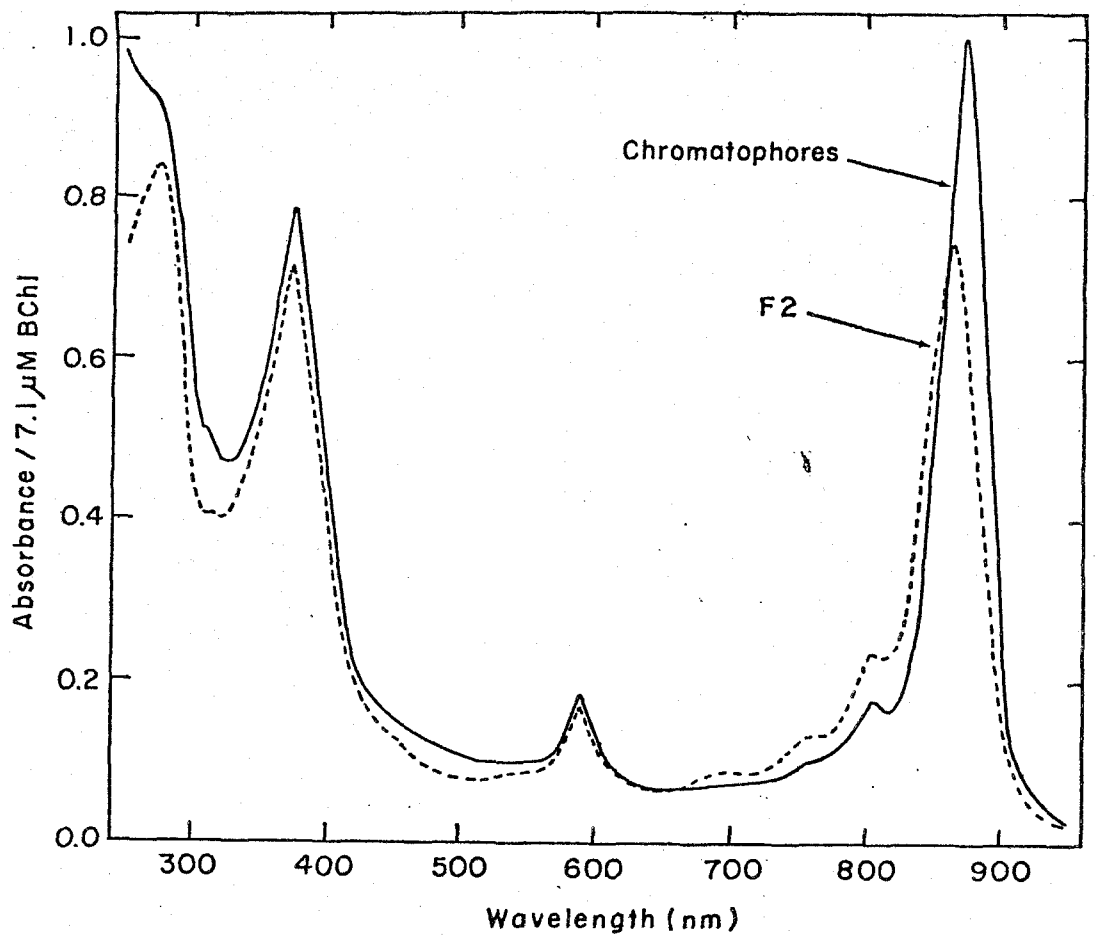

Fig. I-7. Absorbance spectra of chromatophores and purified F2. A preparation of purified F2 was dissolved in 0.05 M Tris-HCl buffer containing 0.1% cholate and 0.3% deoxycholate (pH 8.0); chromatophores were suspended in 0.1 M Tris-HCl buffer. (Nishi *et al.*, 1979)

4 atoms of iron and 90 phosphate groups in each protein complex (Table I-1). In SDS-polyacrylamide concentration-gradient slab gel electrophoresis, the purified F2 was separated into approximately 10 kinds of major protein species, significantly fewer than were obtained with chromatophores (Fig. I-8). The apparent molecular weights of the protein species were 3.8×10^4, 3.6×10^4, 3.5×10^4, 2.8×10^4, 2.7×10^4, 2.6×10^4, 1.3×10^4, 1.2×10^4, 1.1×10^4 and 1.0×10^4 daltons (Fig. I-8). In these protein species, those with molecular weights, 2.8×10^4, 2.7×10^4 and 2.6×10^4 are regarded as those of reaction center, indicating that the F2 possesses reaction center complexes. The purified F2 has no phospholipids (Nishi *et al.*, 1979), whereas chromatophore contains phosphatidylcholine, phosphatidylglycerol, cardiolipin and phosphatidylethanol-amine (Haverkate, Teulings & van Deenen, 1965; Nishi *et al.*, 1979). These results shows that F2 is complexes of proteins and bacteriochlorophylls, and the moderate-angle diffraction patterns really come from protein assembly.

F2 exhibited the same level of reaction center activity as chromatophores (Table I-1). However, this fraction did not possess oxidation-reduction components such as cytochromes and ubiquinone-10 (Nishi *et al.*, 1979). These facts suggest that F2 is the photoreaction unit which contains light-harvesting bacteriochlorophyll protein complexes and a reaction center.

TABLE I-1

COMPARISON OF COMPONENTS AND ACTIVITIES OF CHROMATOPHORES AND PURIFIED F2 (PHOTOREACTION UNITS).

Components and activity	Chromatophore	Purified F2
Ubiquinone-10 (molecules)	308	0.3
Phosphate, total (molecules)	5,000	90
Iron, total (atoms)	280	4
Reaction center activity/7.1 μM BChl	0.01	0.01
Bacteriochlorophyll (molecules)	790	33
Weight in daltons:		
Total	2.5×10^7	7×10^5
Protein + Bacteriochlorophyll	2.2×10^7	7×10^5
Phospholipids	0.3×10^7	0
Photoreaction units (number/chromatophore)	24	

(Nishi *et al.*, 1979)

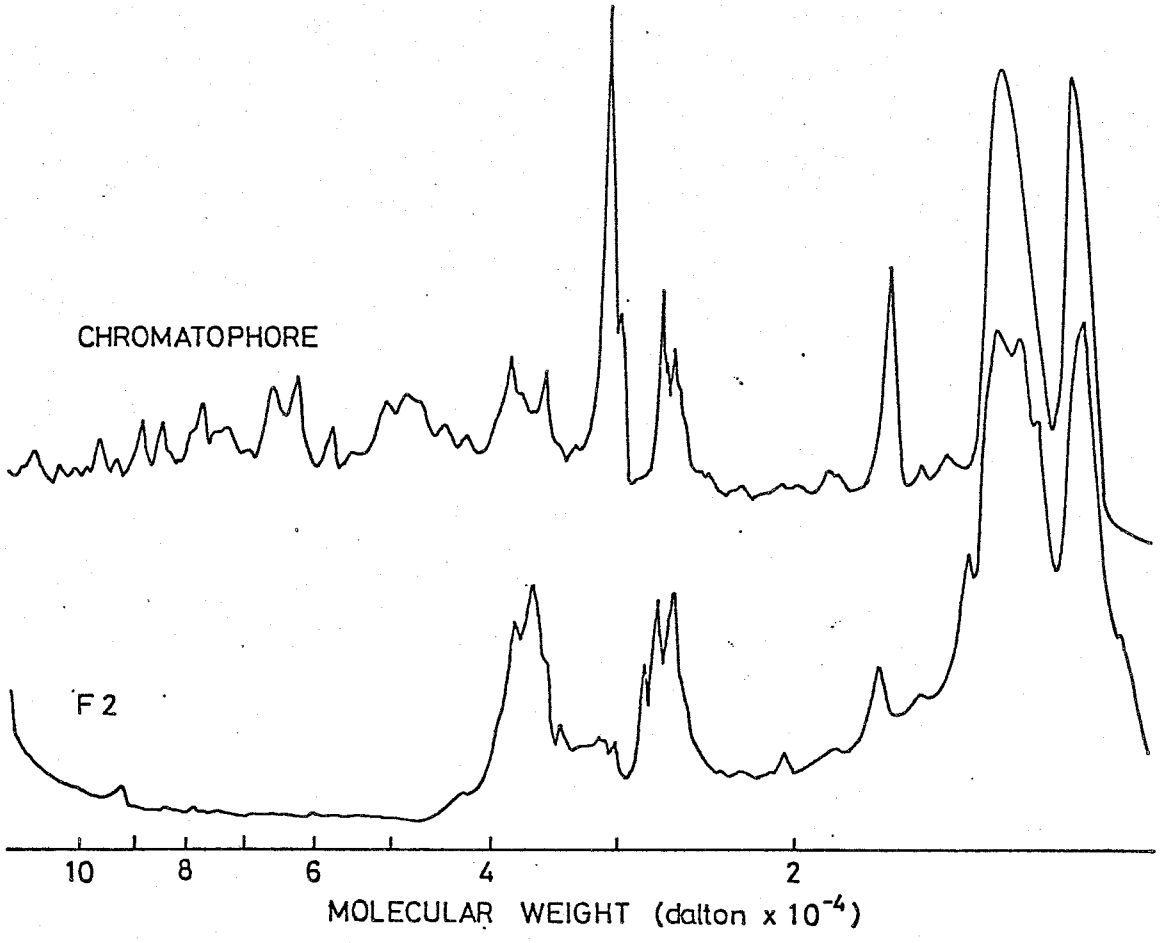

Fig. I-8. SDS-polyacrylamide concentration-gradient slab gel electrophoresis of chromatophore and F2. The stained gel slab was dried under a vacuum to give a thin film, and scanned at 670 nm with a Shimadzu CS-910 dual-wavelength TLC scanner.

(d) Reconstitution of the X-ray Scatterer.

We have already pointed out that some components were removed from the X-ray scatterer in the process of isolation and purification of F2, the photoreaction unit. There are some suggestive experimental results (Nishi *et al.*, 1979): crude F2 contains ubiquinone-10 proteins while purified F2 does not; F3, the reaction center, contains cytochrome c_2 while F2 does not.

We tried to reconstitute the X-ray scatterer from F2, ubiquinone-10 protein and cytochrome c_2. Three reconstituted systems were examined by X-ray diffraction experiment: RS1 is a mixture of F2, ubiquinone-10 protein, cytochrome c_2 and polar lipids; RS2 is a mixture of F2 and polar lipids; RS3 is a mixture of F2, ubiquinone-10 protein and cytochrome c_2, but without polar lipids. X-ray diffraction patterns from RS1, RS2 and RS3 are shown in Fig. I-9. Diffraction maxima at $d \simeq 18\text{Å}$ cannot be observed for RS2 and RS3, but it is clearly visible for RS1. These facts suggest that polar lipids are necessary to reconstitute the X-ray scatterer from F2, though the reconstitution is not performed only with F2 and polar lipids. The fact that RS1 restores the diffraction pattern while RS3 does not, suggest that the X-ray scatterer in chromatophore is the photoreaction unit bound by the oxidation-reduction components. There appears additional diffraction ring inside of 18Å reflection for RS1.

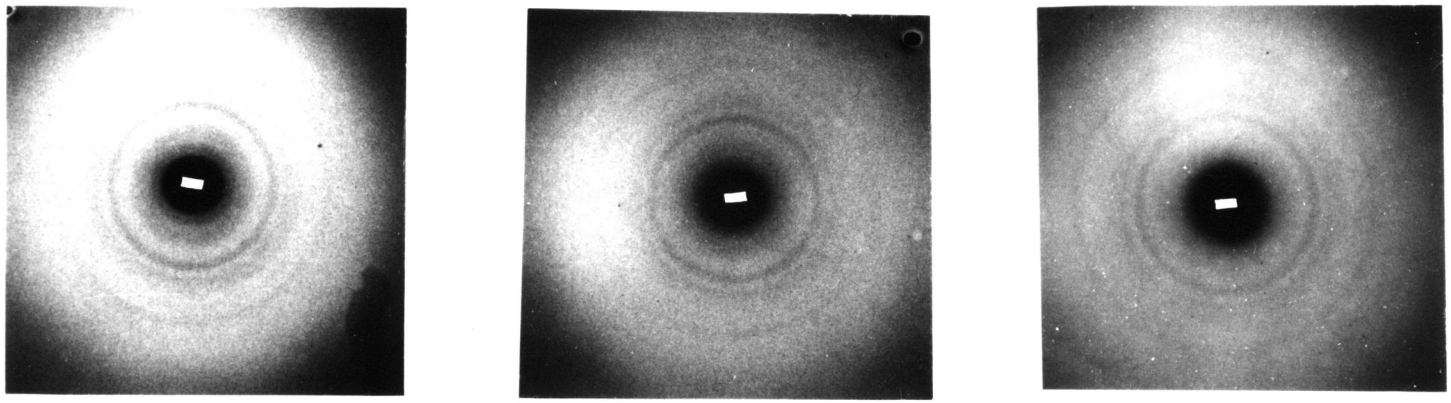

(a) (b) (c)

Fig. I-9. X-ray diffraction photographs of reconstituted systems. (a) RS1, (b) RS2 and (c) RS3.

This ring is considered to be due to polar lipids, because the diffraction pattern from RS2 has the same additional ring while the main features of diffraction pattern are similar to that of F2.

Comparison of moderate-angle diffraction profile of purified F2, RS1, RS2 and chromatophore is shown in Fig. I-10. Diffraction maxima at $d \approx 18\text{Å}$ and 10.5Å are restored for RS1 to the same level as those of chromatophore, while RS2 does not. No appreciable differences are observed in the profiles of RS1 and chromatophore, indicating that ubiquinone-10 protein and cytochrome c_2 are properly attached to the photoreaction unit and reconstitution of the X-ray scatterer is performed.

Photoreaction activities of chromatophore, F2 and RS1 are listed in Table I-2 (Matsuda, Kakuno & Horio, 1980). Photo-oxidation of cytochrome c_2 and photo-reduction of ubiquinone-10 are restored in RS1, while F2 shows no activities. In the case of chromatophore, the activity of photo-oxidation of cytochrome c_2 cannot be measured because the amount of cytochrome c_2 in native chromatophore is too small to detect the absorbance change. Antimycin A is an inhibitor, suppressing the reduction of cytochrome c_2. Therefore, increases of both activities of photo-oxidation of cytochrome c_2 and photo-reduction of ubiquinone-10 with antimycin A indicate that the cyclic electron flow is generated in RS1. We can conclude that the reconstituted

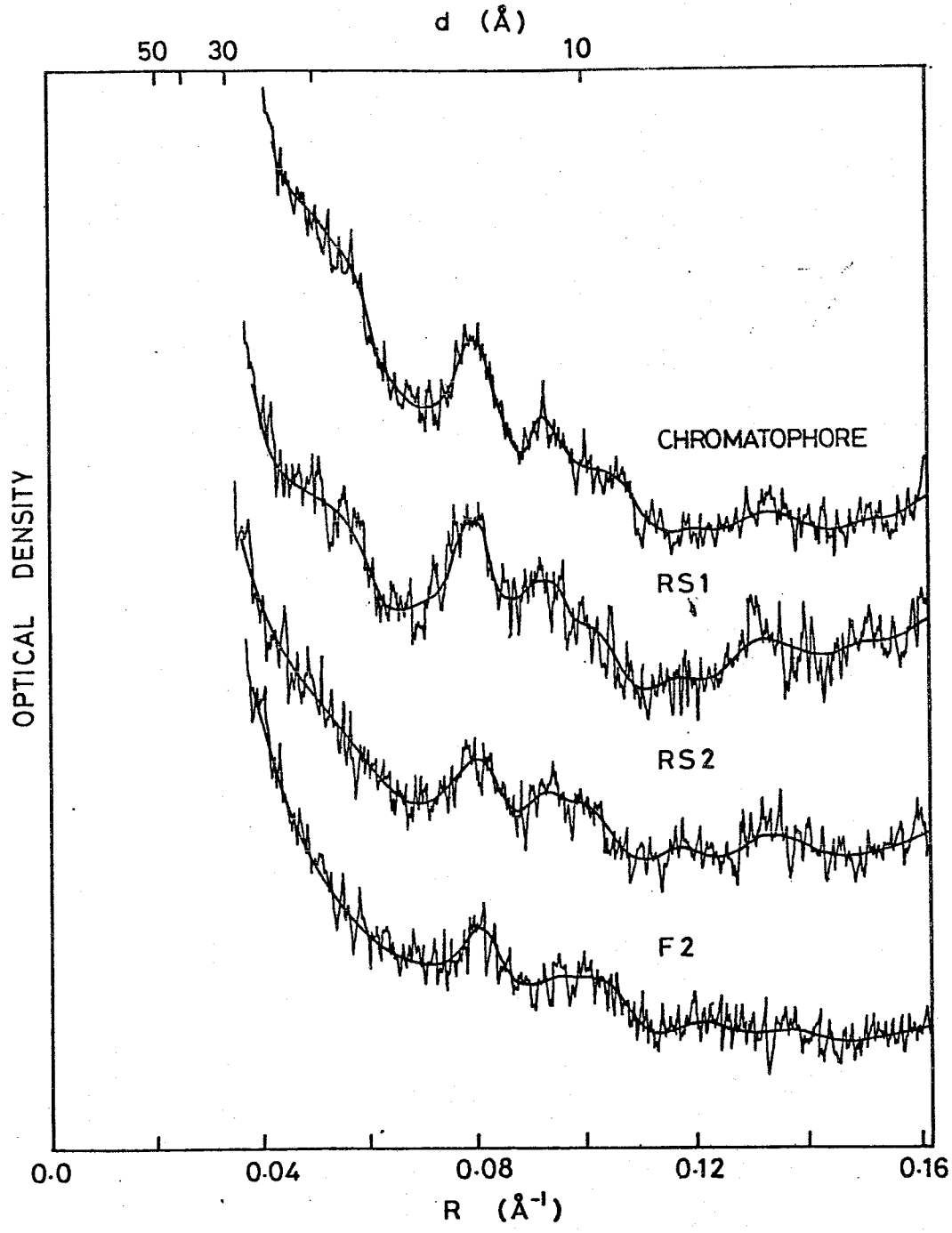

Fig. I-10. Densitometer traces of X-ray photographs from chromatophore, purified F2, and reconstituted systems, RS1 and RS2.

TABLE I- 2

COMPARISON OF PHOTO-REACTION ACTIVITIES OF CHROMATOPHORES, F2, AND RS1

Activity	Chromatophore	F2	RS1[d]
Photo-oxidation of Cyt c_2 [a]			
$-\Delta A_{420nm}$/7.1 μM BChl ($\times 10^3$)			
No addition	-	0	16-17
+ Antimycin A (1 μg/ml)	-	0	47-49
Photo-reduction of UQ-10 [b]			
$-\Delta A_{275nm}$/7.1 μM BChl ($\times 10^3$)			
No addition	3.0	0.1	1.5-1.8
+ Antimycin A (1 μg/ml)	4.5	0.1	4.0-4.8
Reaction center activity [c]			
$-\Delta A_{865nm}$/7.1 μM BChl ($\times 10^3$)			
No addition	10	10	18.1

a) Absorbance change was measured at 15 sec after light-on.

b) Absorbance change was measured at 4 sec after light-on.

c) Absorbance change was measured at 180 sec after light-on.

d) F2:UQ-10 protein:Cyt. c_2: polar lipids = 1:5:5:780

X-ray scatterer, RS1, has the function of the photosynthetic unit. On the other hand, these photoreaction activities were not observed for RS2, and RS3 showed these activities only a quarter of those observed for chromatophore and RS1 (Matsuda, Kakuno & Horio, 1980).

(e) X-ray Diffraction Pattern of Chromatophore Treated with Acetone or Chlorophyllase.

The result obtained previous section that the basic structure of the X-ray scatterer is the photoreaction unit arouses the interest in the role of bacteriochlorophyll molecules. When chromatophores were treated with appropriate concentration of acetone, bacteriochlorophylls were removed from chromatophore (Fig. I-12).

X-ray diffraction patterns from chromatophore treated with various concentration of acetone are shown in Fig. I-11. The moderate-angle diffraction pattern are still observed for 30%-acetone-treated and 50%-acetone-treated chromatophores, but disappears for 70%-acetone-treated chromatophore. In Fig. I-11 (b), the moderate-angle diffraction pattern are mixed with diffuse halo at $d \simeq 10\text{Å}$, which indicates the partial destruction of the regular structure. Critical acetone concentration where the moderate-angle diffraction pattern disappeared is 50 $\sim$ 60%. The structure of the X-ray scatterer is not affected by the treatment with 10 $\sim$ 50% of acetone, however, higher concentrations

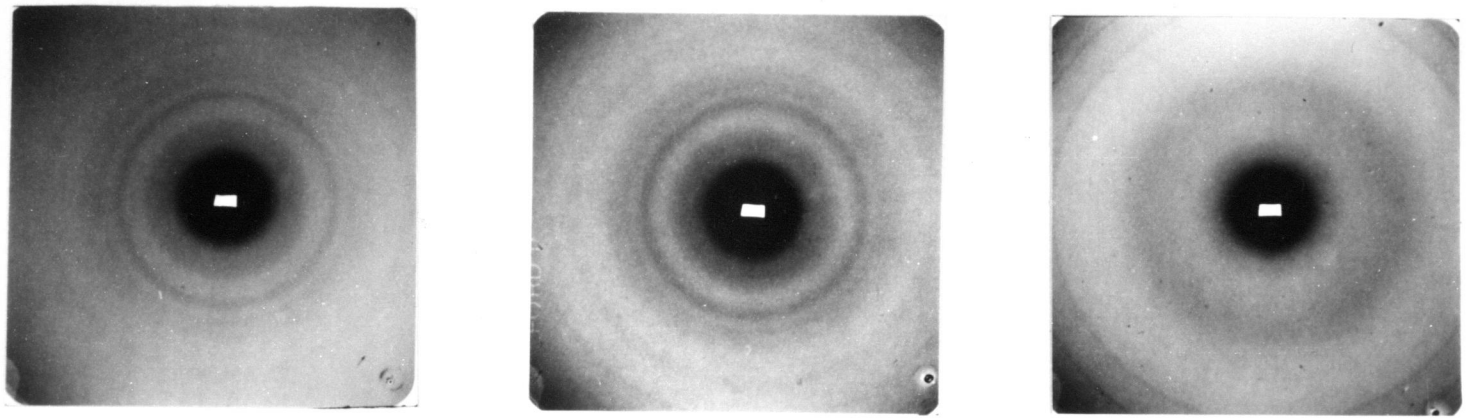

Fig. I-11. X-ray diffraction photographs of chromatophore treated with various concentration of acetone. (a) 30% acetone-treated, (b) 50% acetone-treated and (c) 70% acetone-treated chromatophores.

than 50% of acetone destroy the structure. The sharp 4.2Å reflection due to the crystalline packing of hydrocarbon chains of lipids was observed for the chromatophore treated with 0 ∿ 30% of acetone, but disappeared for more than 50% of acetone-treated chromatophore. This fact suggests that the region occupied by lipids is affected by 50% or higher concentration of acetone. In the cases of 50% or higher concentration of acetone, crystalline reflections are observed at high-angle region, but the origin left unknown.

In Fig. I-12, the effect of acetone on bacteriochlorophyll removal is depicted. Bacteriochlorophylls are not removed at all with 0 ∿ 50%-acetone-treatment. When the concentration exceeded 50%, the abrupt removal of bacteriochlorophyll was observed. Almost all bacteriochlorophylls were removed from chromatophore at acetone concentration of 80%. These behaviours of bacteriochlorophyll removal seem to be in good agreement with the change of diffraction patterns. However, two possible interpretations are derived from these results. The one is that the loss of bacteriochlorophyll causes the deterioration of regular structure; the other is that the structural change cause the removal of bacteriochlorophyll.

When chromatophores were treated with chlorophyllase, bacteriochlorophylls were hydrolyzed to bacteriochlorophyllide and phytol (Tanaka, 1980). The chlorophyllase requires

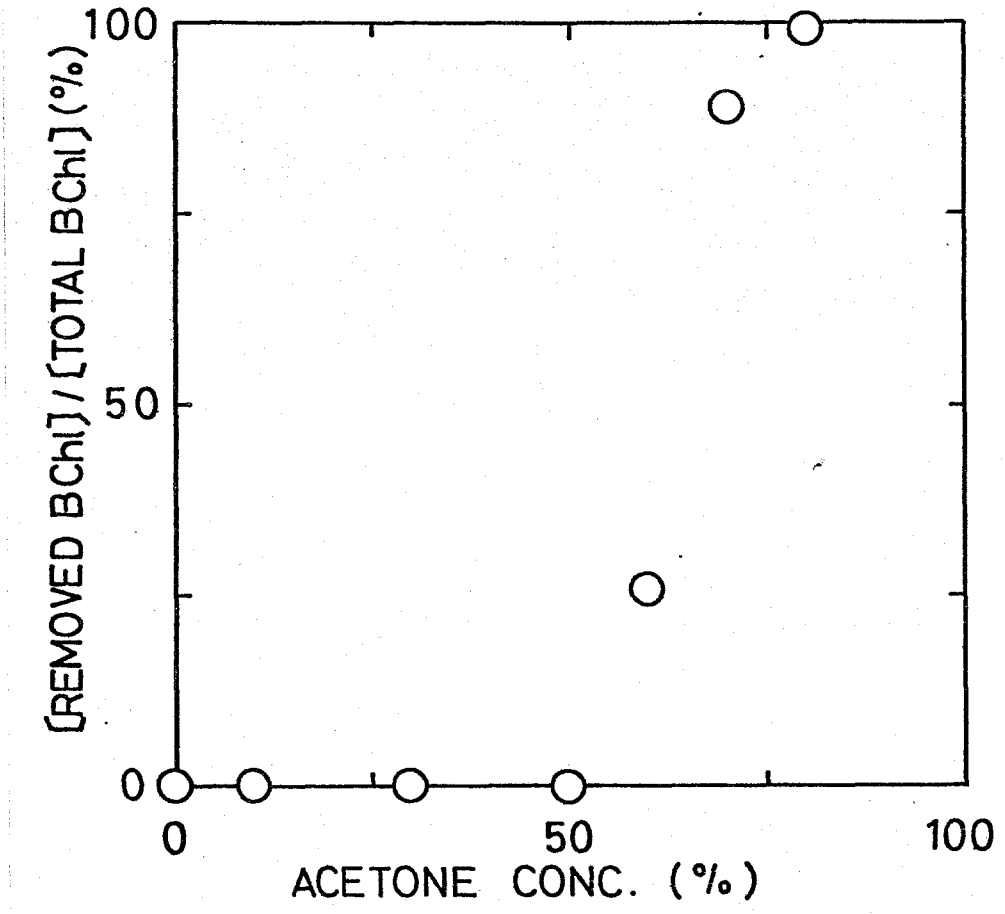

Fig. I-12. Effect of various concentration of acetone on removal of bacteriochlorophyll. The amount of total bacteriochlorophyll is estimated from A_{873nm} (Kakuno *et al.*, 1971).

20 ∿ 30% of acetone for its appearence of activity (Tanaka, 1980). The experiment mentioned above verified that these concentrations of acetone do not show any effect on the structure of the X-ray scatterer, whose basic component is the photoreaction unit. X-ray diffraction patterns from the chromatophore treated with chlorophyllase with various incubation time are shown in Fig. I-13. In Fig. I-14, the time-course of hydrolysis of bacteriochlorophyll by the enzyme is expressed.

At incubation time 5 h, 30% of bound bacteriochlorophylls are hydrolyzed, however, the moderate-angle diffraction pattern is observed without any change. At incubation time 16 h, 80% of bound bacteriochlorophylls are hydrolyzed, and the moderate-angle diffraction almost disappears except for the diffraction maxima around $d \simeq 12\text{Å}$. At incubation time 35 h, almost all bacteriochlorophylls are hydrolyzed, and the moderate-angle diffraction pattern completely disappears and diffuse halo at $d \simeq 10\text{Å}$ becomes clearly visible, indicating that the structure of the X-ray scatterer is already lost and that proteins turn to be randomly distributed. However, when chromatophore was incubated with 20% of acetone without the enzyme for 35 h, the moderate-angle diffraction pattern was maintained without any change, as is shown in Fig. I-13 (d). Moreover, when chromatophore was incubated with the enzyme without acetone, the diffraction pattern

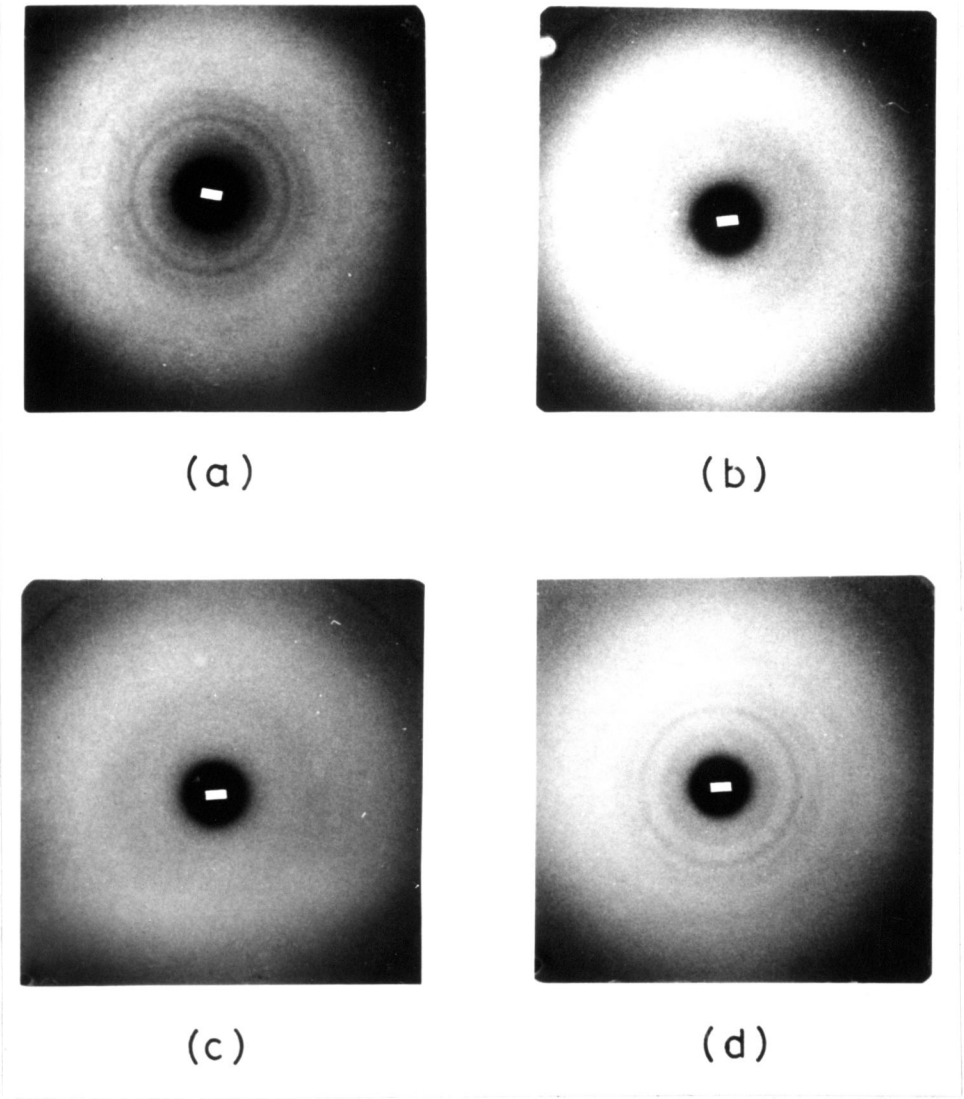

Fig. I-13. X-ray diffraction photographs of chromatophores treated with chlorophyllase with various incubation time. (a) incubation time 5 h, (b) incubation time 16 h, (c) incubation time 35 h and (d) control (incubated in 20% acetone for 35 h without the enzyme). Sharp reflection observed at corners is 4.2Å reflection.

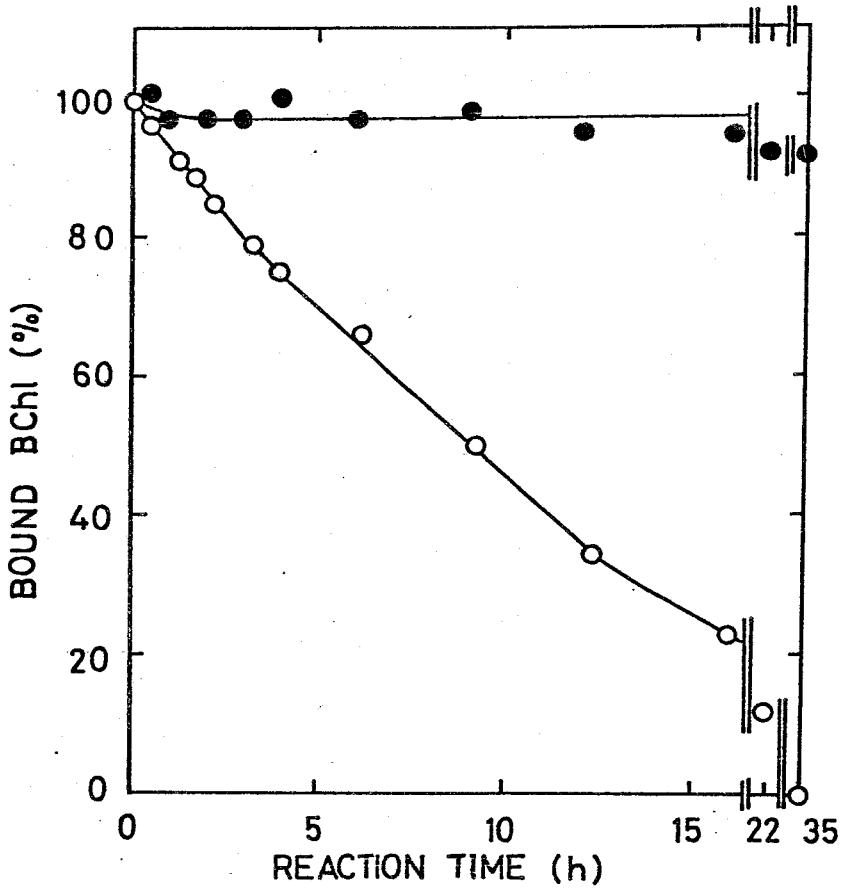

Fig. I-14. Time course of hydrolysis of bacteriochlorophyll by chlorophyllase. The standard reaction mixture containing chlorophyllase (O) or heated chlorophyllase (●) was incubated in the presence of 20% acetone. The ratio of bound bacteriochlorophyll was estimated from the ratio of A_{870nm} at various reaction time and at initial state. (Tanaka, 1980)

stayed unchanged. These results indicate that the hydrolysis of bacteriochlorophylls influences seriously the structure of the X-ray scatterer and, of course, that of the photoreaction unit.

On the other hand, 4.2Å reflection is clearly observed for all cases, indicating that the region occupied by lipids is not affected by the enzyme. In other words, membrane structure of chromatophore is maintained during the treatment with the enzyme.

I-4. DISCUSSION

(a) Identification of the X-ray Scatterer.

By a mixture of cholate and deoxycholate, the photoreaction unit was solubilized from chromatophore, which contains light-harvesting bacteriochlorophyll proteins and a reaction center but does not possess oxidation-reduction components. Chromatophore and the isolated photoreaction unit gave the same diffraction maxima in their profiles. This fact indicated that the X-ray scatterer in the chromatophore is based on the photoreaction unit. It is to be emphasized that the isolation of the photoreaction unit without structural change is verified by the X-ray diffraction studies.

When the photoreaction unit, F2, was treated with

N, *N'*-dimethyllaurylamine oxide (LDAO) which is a widely used detergent, reaction centers were dissociated from the units (N. Nishi & T. Horio, personal communication). The LDAO-treated photoreaction unit, which lacks a reaction center, no longer gave the distinct diffraction pattern (M. Kataoka, unpublished result). Therefore, a reaction center as well as the light-harvesting bacteriochlorophyll proteins plays an important role to construct a rigid and highly organized structure of the X-ray scatterer.

There observed changes in diffraction patterns from chromatophore, crude F2 and purified F2: decreases of intensities of diffraction maxima at $d \simeq 18\text{Å}$ and 10.5Å. These differences do not necessarily mean that they have completely different structures, because differences were only decreases of relative intensities of peculiar diffraction maxima leaving others unchanged. The intensities at these diffraction angles decreased as the purification process proceeded, and hence it was expected that the isolation and purification resulted in removal of certain components. If we can find the removed components, the X-ray scatterer may be reconstituted from the photoreaction unit.

In fact, the X-ray scatterer was reconstituted from photoreaction unit (F2), ubiquinone-10 protein, cytochrome c_2 and total polar lipids. Relative intensities at $d \simeq 18\text{Å}$ and 10.5Å of the reconstituted system are restored to

the level of those of chromatophore (Fig. I-10). The reconstituted system gave the same diffraction profiles as chromatophore, indicating that the X-ray scatterer of chromatophore is completely reconstituted. On the other hand, a mixture of F2, ubiquinone-10 protein and cytochrome c_2 did not restore the diffraction pattern. These facts indicate that the X-ray scatterer consists of photoreaction unit with loosely bound oxidation-reduction components such as ubiquinone-10 protein and cytochrome c_2.

(b) Proofs of the Existence of the Photosynthetic Unit.

The concept of the photosynthetic unit has been generally accepted. In fact, photosystem I and photosystem II have been isolated from chloroplasts (Wessels, 1963; Ogawa *et al.*, 1966; Huzisige *et al.*, 1969; Ohki & Takamiya, 1970), indicating the existence of photosynthetic units in chloroplast. Nishimura (1970) pointed out that the photosynthetic unit of photosynthetic bacteria contains 20 ∿ 40 bacteriochlorophylls, but this bacterial photosynthetic unit has not been isolated. We have already pointed out the possibility of reconstitution of the photosynthetic unit from photoreaction unit and oxidation-reduction components (Nishi *et al.*, 1979).

When photoreaction unit, F2, was mixed with ubiquinone-10 protein and cytochrome c_2 with the aid of polar lipids, the activity of cyclic electron flow could be observed

(Matsuda, Kakuno & Horio, 1980). This fact indicated that, at the least, the function of the photosynthetic unit was reconstituted. Only from the result, however, we cannot decide whether the reconstitution of the unit is completed or not, and thus whether the photosynthetic unit exists in chromatophore.

We have revealed that the reconstituted system, RS1, gave the same diffraction pattern as chromatophore. This fact indicated that the oxidation-reduction components were properly attached to photoreaction unit within RS1, and the structure of RS1 is the same as that of native state. In other words, the functional reconstitution means, at the same time, the structural reconstitution, and the photosynthetic unit was succeeded to reconstitute. Therefore, the existence of the photosynthetic unit in chromatophore is confirmed and the X-ray scatterer is identified as the photosynthetic unit. This finding is important from the viewpoint of function-structure relationship of chromatophore. It is believed so far that a photosynthetic unit may be only a statistical unit which is not always accompanied by a structure counterpart (Arntzen & Briantais, 1975). X-ray diffraction pattern indicates that each component is regularly arranged, not in crystalline manner, in the photosynthetic unit. Each unit has definite and highly organized structure, and contains a part with tight structure (photoreaction unit)

and loosely binding parts (oxidation-reduction components).

(c) Role of Each Component for the Construction of the Photosynthetic Unit.

(i) Bacteriochlorophyll.

With chlorophyllase-treatment, bound bacteriochlorophyll was hydrolyzed to bacteriochlorophyllide and phytol (Tanaka, 1980). Although phytol left in chromatophore, bacteriochlorophyllide is liberated from chromatophore (Tanaka, 1980). When almost all of bacteriochlorophylls were hydrolyzed, the moderate-angle diffraction pattern disappeared completely. These facts suggest that bacteriochlorophylls play important roles to maintain the structure of the photosynthetic unit, and that there are strong interactions between porphyrin rings.

It is well-known that the purple membrane of *Halobacterium halobium* is different type of photosynthetic membrane, and composed of crystalline arrangements of bacteriorhodopsin. The major pigment of the purple membrane is retinal instead of bacteriochlorophyll. In order to construct the crystalline arrangement, retinal is indispensable (Hiraki, Hamanaka, Mitsui & Kito, 1978). The correspondence of the fact that bacteriochlorophyll decides the structure of chromatophore and that retinal decides the structure of the purple membrane is considerably interesting in connection with light-energy conversion.

(ii) Ubiquinone-10.

When chromatophore is treated with *iso*-octane, ubiquinone-10 is extracted (Okayama, Yamamoto, Nishikawa & Horio, 1968). X-ray diffraction pattern of the ubiquinone-10-extracted chromatophore was not appreciably different from that of native chromatophore (Kataoka, 1976; Ueki *et al.*, 1976). This fact suggests that molecules of ubiquinone-10 are not concerned with the preservation of the structure of the photosynthetic unit. However, the molecules of ubiquinone-10 bind with proteins and are considered to be located in the fixed positions in the photosynthetic unit.

(iii) Lipids.

Although the photoreaction unit does not possess phospholipids (Nishi *et al.*, 1979), polar lipids play active parts in the construction of the photosynthetic unit. There are several lines of evidence.

(1) Polar lipids were indispensable to reconstitute the X-ray scatterer from the photoreaction unit and oxidation-reduction components.

(2) The absorbance spectrum of the photoreaction unit shows the main peak due to bacteriochlorophyll at 865 nm which is 8 nm shorter than that of chromatophore. This peak is recovered to 871 nm when polar lipids were added to the photoreaction unit (Matsuda *et al.*, 1980).

(3) Photoreaction activities were observed for RS1, which is reconstituted photosynthetic unit, while the reconstituted system without polar lipids, RS3, did not show the activities (Matsuda *et al.*, 1980).

Moreover, sharp 4.2Å reflection which is occasionally observed indicates that lipids construct the basic membraneous structure of chromatophore, as is expected from the fluid-mosaic model (Singer & Nicolson, 1972).

(iv) Carotenoids.

The chromatophore of wild *R. rubrum* which possesses carotenoids gave the same diffraction pattern as that of blue-green mutant (M. Kataoka, unpublished result). The photoreaction unit isolated from wild cells contains carotenoids (Nishi *et al.*, 1979). These facts suggest that carotenoids do not play roles in maintaining the structure of the photosynthetic unit, even though they are included in the unit.

(d) Comparison with the Other Photosynthetic Bacteria.

Comparative X-ray studies revealed that chromatophores of typical photosynthetic bacteria give distinct X-ray diffraction patterns, which are, however, different from that of *R. rubrum* chromatophore (Inai, 1980; Inai, Kataoka & Ueki, 1980). All photosynthetic bacteria which we examined have definite and highly organized structure in their

chromatophore membrane, presumably the photosynthetic unit. X-ray diffraction patterns from chromatophores of *R. rubrum*, *Rps. sphaeroides*, *Chromatium vinosum* and *Chlorobium thyosulfatophilum* which are typical photosynthetic bacteria are shown in Fig. I-15. X-ray diffraction patterns from various bacterial chromatophores can be classified into four groups (Inai, 1980; Inai *et al.*, 1980). These differences correspond well to the differences of absorbance spectra due to bacteriochlorophyll. This fact suggests that the internal structure of the photosynthetic unit is varied from species to species, and is defined by the state of light-harvesting bacteriochlorophylls.

I-5. SUMMARY

Results obtained by the studies described in this chapter may be summarized as follows.

(1) Chromatophores isolated from photosynthetic bacterium, *Rhodospirillum rubrum*, give distinct X-ray diffraction pattern in the equatorial direction, which indicate the existence of highly organized structure (X-ray scatterer) in the membrane plane.

(2) The basic component of the X-ray scatterer is solubilized from chromatophores with a mixture of cholate

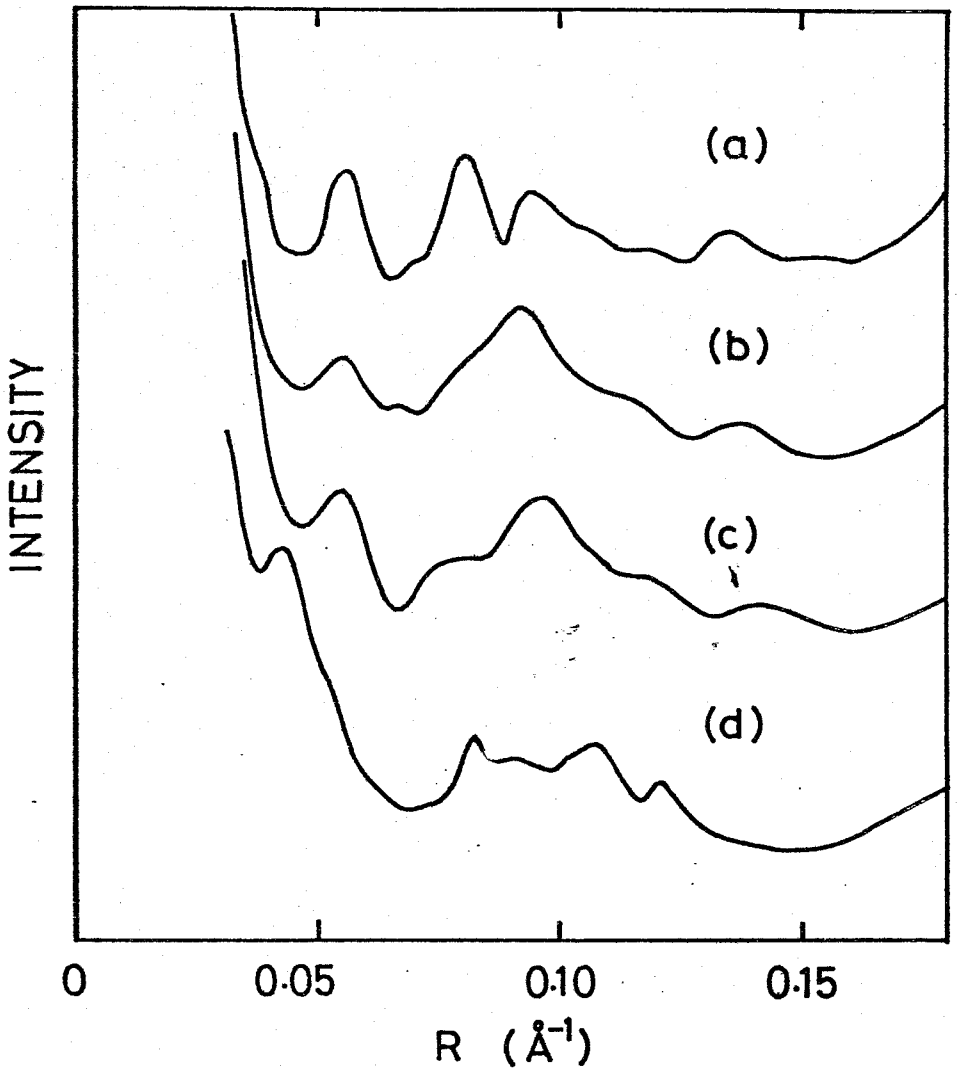

Fig. I-15. Equatorial X-ray diffraction profiles of photosynthetic apparatuses from various photosynthetic bacteria. (a) *R. rubrum*, (b) *Rps. sphaeroides*, (c) *Ch. vinosum* and (d) *C. thiosulfatophilum*. (Inai, 1980)

and deoxycholate, and is identified as the photoreaction unit which contains light-harvesting bacteriochlorophyll protein complexes and a reaction center.

(3) The X-ray scatterer is reconstituted from the isolated photoreaction unit, oxidation-reduction components (ubiquinone-10 protein and cytochrome c_2) and polar lipids. Polar lipids are essential to reconstitute the X-ray scatterer. The reconstituted X-ray scatterer possesses the function of the photosynthetic unit: the X-ray scatterer is the photosynthetic unit.

(4) When more than 90% of bound bacteriochlorophyll molecules are hydrolized by chlorophyllase, the structure of the photosynthetic unit is lost.

CHAPTER II

RADIAL AUTOCORRELATION FUNCTION
AND
THE STRUCTURAL FEATURES OF THE PHOTOSYNTHETIC UNIT

II-1. INTRODUCTION

As was mentioned in Chapter I, we have obtained continuous X-ray diffraction patterns in the equatorial direction from the oriented specimens of chromatophore, which were revealed to arise from the photosynthetic unit. Our problem to solve next is how constituent molecules are arranged in the photosynthetic unit. Apart from chromatophore, the continuous equatorial X-ray diffraction patterns have been obtained from some biomembranes: outer membranes of *Salmonella typhimurium* and *Escherichia coli* (Ueki *et al.*, 1976; Ueki *et al.*, 1979; Ueki *et al.*, 1980); outer membrane of plant mitochondria (Mannella & Bonner, 1975); electroplaque of *Torpedo* (Dupont *et al.*, 1974); thylakoid membrane of blue-green alga and chloroplast from spinach (Tsukamoto *et al.*, 1980). These patterns are caused by regular arrangements of protein molecules in the plane of these membranes. They consist of several diffraction maxima which are much sharper than the "halo" from amorphous materials but broader than the crystalline reflection. It is necessary that we find an effective and decisive method to interpret the equatorial diffraction patterns of these membranes as well as chromatophore.

Since the problem is concerned with the arrangement of protein molecules in X-ray scatterers, the Patterson function is relevant to our purpose. In crystal structure analysis, the Patterson function gives information on the

space group (Buerger, 1951). In the case of membranes, X-ray scatterers are randomly rotated with respect to an axis normal to the membrane surface when they are stacked, and the equatorial intensity is a circular symmetric function depending only on the radial coordinate of the cylindrical polar coordinates. The Patterson function calculated from such a circular symmetrical intensity is called the "radial autocorrelation function". The cylindrically symmetrical Patterson function proposed for fibrous system by MacGillavry and Bruins (1948), which is the same as the radial autocorrelation function in principle, has often been misunderstood to correspond to a cylindrically symmetric structure. However, it was pointed out that the radial autocorrelation function preserves non-circular symmetric components of electron density distribution in the scatterers even if directional components of vectors are lost (Earnshaw, Casjens & Harrison, 1976).

In this chapter, we have developed a strict relation between the radial autocorrelation function and the electron density distribution. The equatorial diffraction pattern from chromatophore was interpreted by the radial autocorrelation function and some structural features were obtained.

II-2. EXPERIMENTAL PROCEDURES

(a) X-ray Diffraction Experiment.

The procedures were completely the same as described in previous chapter. Dried specimen of chromatophore was used and X-ray beam was incident parallel to the membrane plane.

(b) Intensity Data.

The optical density of diffraction photograph was measured with a Nalumi C-type microdensitometer and converted to intensity data by using the calibrated intensity scale. The intensity data after subtraction of background scattering were corrected for the Lorentz factor, $\lambda/2\sin\theta$, to obtain the intensity function, $I_0(R)$, where 2θ, λ and R $(=2\sin\theta/\lambda)$ are the diffraction angle, the X-ray wavelength and the reciprocal radial coordinate, respectively.

Background scattering was estimated as follows. By comparison of equatorial diffraction from the oriented specimen and diffraction pattern from the wet specimen (see Fig. I-2), smooth and simple background was drawn so that intensities at $d \simeq 23\text{Å}$ and 15Å and $d < 6.2\text{Å}$ became zero.

(c) Calculations.

All the calculations were carried out by ACOS-S700 computer of Crystallographic Research Center at Institute

for Protein Research, Osaka University.

II-3. ANALYTICAL PROCEDURES

(a) Fundamental Equations.

In this chapter, X-ray diffraction is discussed in terms of cylindrical polar coordinates. Two-dimensional vectors, (r,ϕ) and (R,Φ), are used in real and reciprocal spaces, respectively. Vector (u,χ) is used in vector space.

We take a unique axis ($\mathbf{z}$) of membrane parallel to the membrane normal. An equatorial diffraction from the membrane corresponds mathematically to an electron density projection along $\mathbf{z}$. Thus, the X-ray scatterer which is related to the observed intensity, $I(R,\Phi,0)$, is the electron density projection $\sigma(r,\phi)$ of the protein assembly on the membrane matrix.

$$I(R,\Phi,0) = \left|\iiint \rho(r,\phi,z)\exp[-2\pi irR\cos(\phi-\Phi)]\,r\,dr\,d\phi\,dz\right|^2$$

$$= \left|\iint \sigma(r,\phi)\exp[-2\pi irR\cos(\phi-\Phi)]\,r\,dr\,d\phi\right|^2$$

$$\equiv I(R,\Phi) \qquad (1)$$

where

$$\sigma(r,\phi) = \int \rho(r,\phi,z)\,dz.$$

In the X-ray specimens of biomembranes, all the rotational orientations of scatterers are equally probable about z axis. Then, the observed equatorial intensity is a circular symmetrical function, $I_0(R)$, instead of $I(R,\Phi)$. $I_0(R)$ is obtained through the integration of $I(R,\Phi)$ with Φ as,

$$I_0(R) = \sum_n |F_n(R)|^2 \tag{2}$$

where

$$F_n(R) = \exp(-in\tfrac{\pi}{2}) \int \sigma_n(r) J_n(2\pi rR)\, 2\pi r dr. \tag{3}$$

J_n is the Bessel function of order n (Waser, 1955; Franklin & Klug, 1955). In the equation, $\sigma_n(r)$ is the Fourier coefficient in the expansion of $\sigma(r,\phi)$ with respect to ϕ and is given by,

$$\sigma_n(r) = \frac{1}{2\pi}\int \sigma(r,\phi)\exp(in\phi)\, d\phi. \tag{4}$$

A radial autocorrelation function $A_0(u)$ is given by the inverse Fourier-Bessel transform of $I_0(R)$ (MacGillavry & Bruins, 1948):

$$A_0(u) = \int I_0(R) J_0(2\pi Ru)\, 2\pi R dR. \tag{5}$$

It is important to point out that $A_0(u)$ is the first term in the Fourier expansion of $A(u,\chi)$ with respect to azimuth χ and is to be understood as the radial projection of $A(u,\chi)$. Therefore, $A_0(u)$ must be discussed on the basis

of the two-dimensional autocorrelation function $A(u,\chi)$ of the structure in conjunction with the arrangement of molecules in the scatterer. In general, an electron density projection, $\sigma(r,\phi)$, can be expressed by summation of electron density fluctuations. (As an example, the structure of a trimer of bacteriorhodopsin from purple membrane is shown in Fig. II-6.) Vectors between fluctuations are represented in $A(u,\chi)$, that is, the disposition function of fluctuations determines peak positions in $A(u,\chi)$ and thus $A_0(u)$. Especially in the case of crystals, disposition function is a lattice function. We must have appreciable peaks in $A_0(u)$ which correspond to the vectors of the lattice points in a crystalline structure: for instance, if the equatorial diffraction pattern is from a two-dimensional hexagonal structure, we must observe large peaks at $u = a$, $\sqrt{3}a$, $2a$, and so on (a being the cell edge).

(b) Radial Autocorrelation Function and Electron Density Fluctuation.

As was pointed out by MacGillavry and Bruins (1948), $A_0(u)$ is not calculated from the self-convolution of circular symmetrical electron density, $\sigma_0(r)$. This point can be clearly shown by the next equation which is derived from Eqs. (2) and (5):

$$A_0(u) = \sum_n \left| \int F_n(R) \right|^2 J_0(2\pi Ru)\, 2\pi R dR$$

$$= \sum_n a_n(u). \qquad (6)$$

Each $a_n(u)$ can be discussed on the basis of the Fourier components of electron density fluctuation, as follows.

In order to clarify the physical meaning, we represent the complex Fourier coefficient $\sigma_n(r)$ in terms of the modulus $|\sigma_n(r)|$ and phase $\alpha_n(r)$. Then, $\sigma(r,\phi)$ can be expressed by (Vainshtein, 1966),

$$\sigma(r,\phi) = \sigma_0(r) + 2 \sum_{n>0} |\sigma_n(r)| \cos\{n\phi+\alpha_n(r)\}. \qquad (7)$$

The n-th component represents the electron density fluctuation with n-fold rotational symmetry and its Fourier transform, $F_n'(R,\Phi)$, is related to $F_n(R)$ by Eq. (3) as,

$$F_n'(R,\Phi) \equiv \mathsf{F}[2|\sigma_n(r)|\cos\{n\phi+\alpha_n(r)\}]$$

$$= \begin{cases} 2|F_n(R)|\cos\{n\Phi+\beta_n(R)\} & (n;\ \text{even}) \\ 2i|F_n(R)|\sin\{n\Phi+\beta_n(R)\} & (n;\ \text{odd}) \end{cases} \qquad (8)$$

where F denotes the Fourier transform and $\beta_n(R)$ is the phase of $F_n(R)$. The Fourier transform of $|F_n'(R,\Phi)|^2$ is equal to the self-convolution of the n-fold rotational symmetrical component of $\sigma(r,\phi)$ as is well known from the multiplication theorem of Fourier integral.

$$\mathsf{F}[|F_n'(R,\Phi)|^2] = 2|\sigma_n(r)| \widetilde{\cos\{n\phi+\alpha_n(r)\}}^2$$

$$= a_n'(u,\chi) \tag{9}$$

where $\overset{2}{\sim}$ denotes the self-convolution operation. $a_n'(u,\chi)$ is a two-dimensional function with 2n-fold rotational symmetry given by

$$a_n'(u,\chi) = \begin{cases} 4\iint |F_n(R)|^2 \cos^2\{n\Phi+\beta_n(R)\}\exp[2\pi iRu\cos(\Phi-\chi)] \\ \times RdRd\Phi \qquad (n;\ \text{even}) \\ \\ 4\iint |F_n(R)|^2 \sin^2\{n\Phi+\beta_n(R)\}\exp[2\pi iRu\cos(\Phi-\chi)] \\ \times RdRd\Phi \qquad (n;\ \text{odd}) \end{cases}$$

$$= 2[\int |F_n(R)|^2 J_0(2\pi Ru)\,2\pi RdR + Re[\exp(i2n\chi) \times \int |F_n(R)|^2 \exp\{i2\beta_n(R)\}J_{2n}(2\pi Ru)\,2\pi RdR]]. \tag{10}$$

where Re denotes the real part of a complex number. Upon integration of Eq. (10) with respect to χ to obtain the radial projection of $a_n'(u,\chi)$, we have

$$\langle a_n'(u,\chi)\rangle_\chi = 2\int |F_n(R)|^2 J_0(2\pi Ru)\,2\pi RdR$$

$$= 2a_n(u).$$

Therefore,

$$a_n(u) = \frac{1}{2}\langle a_n'(u,\chi)\rangle_\chi. \tag{11}$$

Similarly, we can conclude that $a_{-n}(u)$ contributes to $\langle a_n'(u,\chi)\rangle_\chi$ as the other half component.

Equations (9) and (11) show that $a_n(u)$ is the radial autocorrelation function of the component with n-fold rotational symmetry of electron density projection,

$|\sigma_n(r)|\cos\{n\phi+\alpha_n(r)\}$. $a_0(u)$ clearly corresponds to the circular symmetrical electron density $\sigma_0(r)$ and $a_n(u)$ includes information as to the n-fold rotational symmetrical component. If we can extract contributions of each $a_n(u)$ from $A_0(u)$, we have a knowledge on the symmetry element of the X-ray scatterer.

(c) Approach to the Estimation of each $a_n(u)$.

Firstly, we estimate a function $[A_0(u) - a_0(u)]$ by drawing a mean curve through $A_0(u)$, and the function corresponds to

$$[A_0(u) - a_0(u)] = \sum_{n\neq 0} a_n(u). \qquad (12)$$

In Eq. (12), $a_n(u)$ can be discussed on the basis of the n-th Fourier component of electron density fluctuation and its autocorrelation function as is discussed in the above section: for $n = 1$, the structure is of a dipole arrangement; for $n = 2$, the arrangement is quadrupole, and so on. These arrangements of electron density fluctuations give characteristic vectors in $A(u,\chi)$ and hence vector magnitudes in $A_0(u)$. For instance, if we can find a minimum at u_0 and a maximum peak at $\sqrt{2} \times u_0$ in $A_0(u)$, these peaks suggest an arrangement of electron density fluctuations with $n = 2$, and if we find two minima at u_0 and $2 \times u_0$ and one positive maximum at $\sqrt{3} \times u_0$, an arrangement of electron density fluctuations with $n = 3$ is predicted. In Fig. II-1, the

cases with n = 2, 3, 4, 5 and 6 are depicted schematically. As is shown in Fig. II-1, each $a_n(u)$ gives the expected maxima and minima and no other peaks. However, the maximum or minimum at the largest position are slightly shifted to larger u, and the shift increases as n increases. This shift is due to the extent of the electron density fluctuation in radial direction.

Thus, we may find the Fourier components of electron density fluctuations by way of the radial autocorrelation function. Especially, when the scatterer has rotational symmetry, the method of radial autocorrelation function will be quite effective for structure analysis. Adding to it, as is deduced from Fig. II-1, when all $a_n(u)$'s equally contributes to $A_0(u)$, *i. e.*, the scatterer has no spatial correlations, $A_0(u)$ is hardly to have a fine structure.

Fig. II-1 (next page) Schematic picture of $|\sigma_n(r)|\cos(n\phi)$ and corresponding $a_n(u)$ with (a) n = 2, (b) n = 3, (c) n = 4, (d) n = 5 and (e) n = 6, where $|\sigma_n(r)| = \exp[-(1/2)\{(r-r_0)/2.0\}^2]$. Solid line of $|\sigma_n(r)|\cos(n\phi)$ indicates positive value and broken line negative. Symbols + and - represent a maximum and a minimum, respectively. Expected maxima and minima are also indicated in $a_n(u)$.

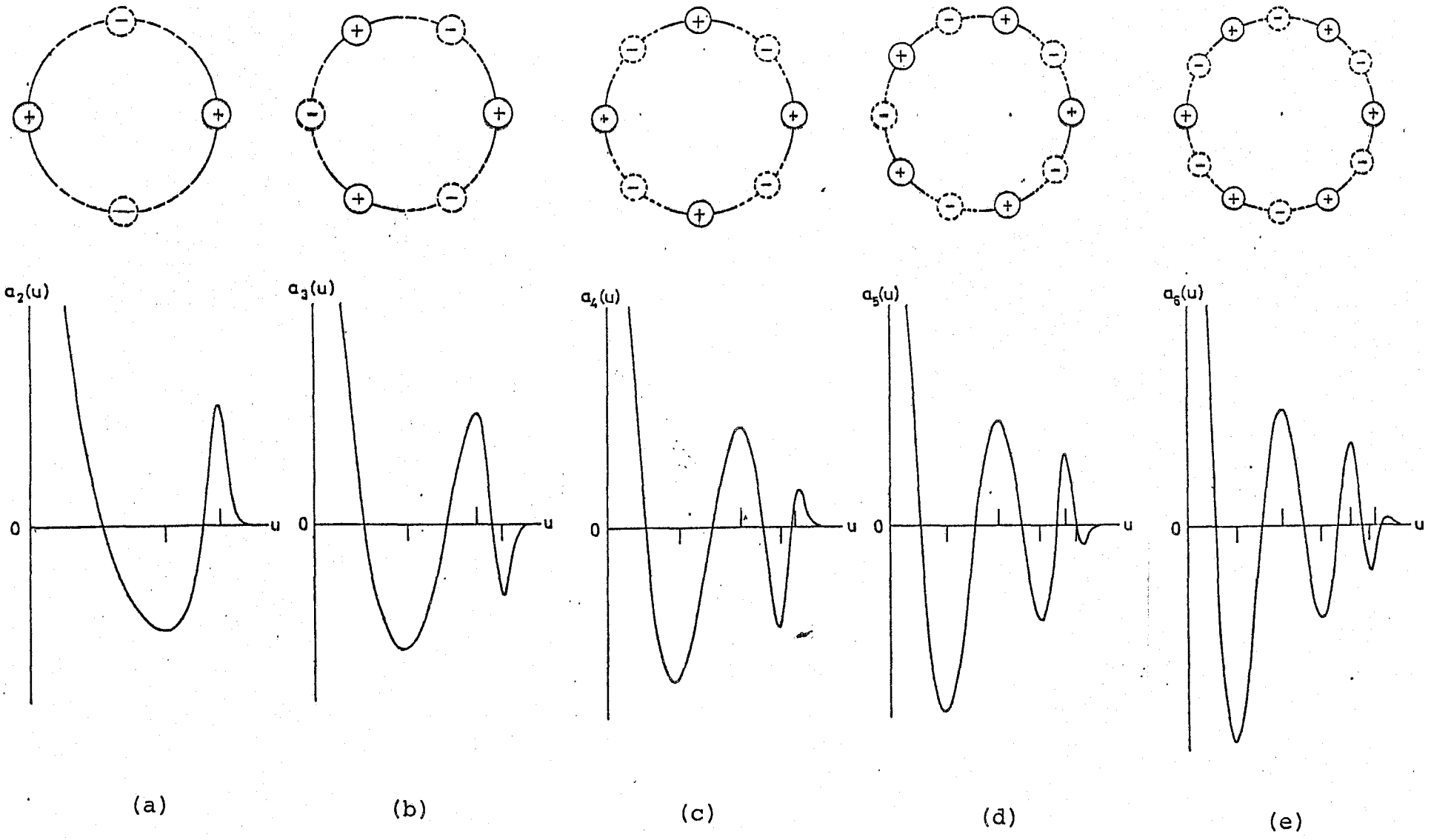

Fig. II-1.

(d) Analysis of Radial Autocorrelation Function.

We can extract useful clues for the structure of scatterer from $A_0(u)$ as below.

(i) The approximate size of the X-ray scatterer is easily estimated, if the scatterer is finite, from the region where $A_0(u)$ approaches zero (Porod, 1951).

(ii) Arrangement of constituent molecules whether it is crystalline or not.

(iii) Fine structure in $A_0(u)$ shows explicitly the existence of electron density fluctuations in the projected $\sigma(r,\phi)$ along the z axis.

(iv) Fine structure in $A_0(u)$ suggests the regular arrangement of electron density fluctuations such as rotational symmetry, because fine fringes in $A_0(u)$ suggest that the contribution of $a_n(u)$ is appreciable.

(v) Contribution of each $a_n(u)$ may be obtained by examination of ratios between maxima and/or minima.

II-4. RESULTS

(a) Is the Photosynthetic Unit a Microcrystal or not?

The equatorial intensity function, $I_0(R)$, of chromatophore is shown in Fig. I-2. These diffraction maxima could be explained by assuming a two-dimensional hexagonal lattice with a = 42.6Å. Calculated spacings of reflections are

compared with the observations in Table II-1. If the indexing is reliable, the line widths would suggest that the crystalline arrangement extends only in a limited area, because the widths do not depend on diffraction angle at all. On the assumption that the protein molecules in the photosynthetic unit form small two-dimesnional crystalline clusters, the observed line width gave the diameter of the cluster as being about 120Å, roughly three times the lattice constant a, on the basis of Scherrer's formula.

However, there have remained some doubts for this assumption. Since there assumed to be three unit cells in each direction, the scatterer consisted of $3 \times 3 = 9$ unit cells. If this interpretation is true, proteins belonging to the central unit cell and those belonging to the surrounding unit cells should have different conformations, because each has different interactions with neighbouring molecules. The latter are also in different conformations to each other. This is hardly to be admitted for the structural model of the X-ray scatterer. Secondly, we have no reason why crystallization ceased at such an early stage. Finally, such a two-dimensional microcrystal was not observed by electron microscopy (Oda & Horio, 1964; Holt & Marr, 1965; Oelze & Golecki, 1975).

The answer for the question whether the photosynthetic unit is a microcrystal or not can be given by a radial

TABLE II-1

OBSERVED AND CALCULATED SPACINGS *d*

FOR EQUATORIAL REFLECTIONS.

h, *k*	*d* (calculated) Å	*d* (observed) Å
0, 1	37.2	——
1, 1	21.0	——
0, 2	18.0	17.9
1, 2	13.8	14.1
0, 3	12.2	12.4
2, 2	10.6	10.5
1, 3	10.1	——
0, 4	9.1	9.4
2, 3	8.4	8.4
1, 4	8.0	——
0, 5	7.3	7.4

A hexagonal lattice with a cell edge of 42.6Å was used for calculation of the spacings. *h*, *k* are Miller indices.

autocorrelation function, $A_0(u)$, calculated from an equatorial intensity function, $I_0(R)$, as is mentioned in the previous section. Peak positions of a radial autocorrelation function express vector magnitudes in the electron density projection within the X-ray scatterer along the membrane normal. If the in-plane structure is really a two-dimensional crystal, the number of vectors whose magnitudes are equal to the cell edge is the highest among all vectors within the scatterer.

The radial autocorrelation function calculated from $I_0(R)$ of chromatophore (Fig. I-2) is shown in Fig. II-2. The peak expected at u = 42.6Å from the assumed unit cell was observed as a small shoulder of the neighbouring peak. The expected peak at u = 73.8Å and at u = 85.2Å which correspond to $\sqrt{3}a$ and $2a$, respectively, were not observed. Therefore, the indexing is concluded to be accidental. The X-ray scatterer, the photosynthetic unit, is not a microcrystal. The equatorial diffraction of chromatophore is, therefore, caused by the internal structure of the particle described in the next section.

(b) Features of the Structure of the Photosynthetic Unit.

The radial autocorrelation function gave a conclusion that the photosynthetic units are randomly distributed in a chromatophore membrane and the internal structure of the unit has some regular arrangements of constituent molecules.

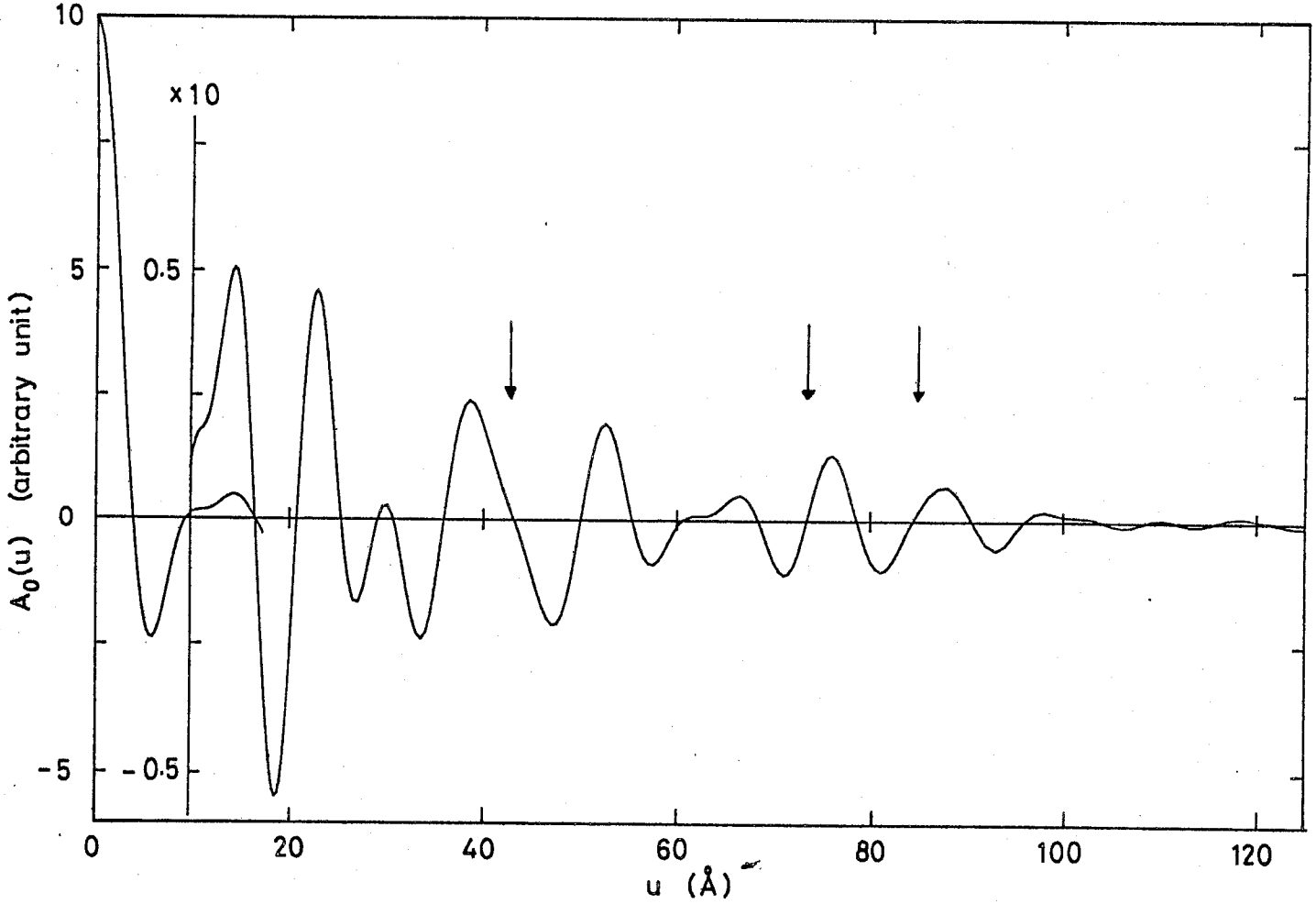

Fig. II-2. Radial autocorrelation function, $A_0(u)$, of chromatophore calculated from equatorial intensity data of oriented specimen. Arrows express the expected peak positions given by the first, second and third neighbours from the assumed cell edge, 42.6Å.

The same situation was observed for porin assemblies existed in the outer membranes of *S. typhimurium* and *E. coli* (Ueki *et al.*, 1979). The regular spatial arrangement of electron densities in a particle gives rise to a distinct, but broad X-ray diffraction pattern as seen in the well-known X-ray diffraction pattern from gaseous carbontetrachloride (van der Grinten, 1932).

The radial autocorrelation function gives some other useful informations about the structure, as is shown in the previous section. $A_0(u)$'s decreased to zero at u = 110 ∿ 130Å for most of the cases. Peak positions of $A_0(u)$'s were consistent within the range of u < 120Å as shown in Fig. II-2. Thus, it is reasonable to conclude that the approximate size of the photosynthetic unit is 110 ∿ 130Å.

The fine structures of $A_0(u)$ indicate that there exist fluctuations in electron density distribution and fluctuations are in regularly arrangement other than crystalline arrangement. In Table II-2, the peak positions observed in the radial autocorrelation function (Fig. II-2) are listed. We could observe three sets of vectors which have ratios of 1, √3 and 2 as is also listed in Table II-2. The vector set with this ratio is, in the simplest case, the characteristics of a regular hexagonal arrangement of molecules in the scatterer. Therefore, we can deduce one possibility that the X-ray scatterer, the photosynthetic unit, has a six-fold rotational symmetry.

TABLE II-2

VECTOR MAGNITUDES, u_i, OBTAINED FROM RADIAL AUTOCORRELATION FUNCTION, $A_0(u)$ AND THE RATIOS OF VECTOR MAGNITUDES

u_i (Å)	ratios u_i/u_0		
	u_0=30.0Å	u_0=38.5Å	u_0=43.5Å
10.0			
14.5			
22.8			
30.0	1.00		
38.5		1.00	
43.5			1.00
52.5	1.75		
61.3	1.98		
66.5		1.73	
76.0		1.99	1.75
87.5			2.01
97.5			
102.5			
110.0			
118.0			

II-5. DISCUSSION

(a) Indexing of Diffraction from the Scatterer with Limited Size.

It is revealed that the photosynthetic unit is not a crystal, although the equatorial reflection could be indexed as a two-dimensional hexagonal lattice. Thus, apparently successful indexing was only by accidental. This is not an exceptional result for chromatophore. There was another example. The oriented specimen of the outer membrane from *S. typhimurium* also gave diffuse but distinct X-ray diffraction in the equatorial direction (Ueki *et al.*, 1976). The equatorial reflection could be indexed as a two-dimensional hexagonal lattice with a = 80Å (Ueki *et al.*, 1979). However, the indexing is concluded to be accidental, since the $A_0(u)$ does not have peaks expected from the assumed lattice (Ueki *et al.*, 1979; Kataoka & Ueki, 1980). The size of the scatterer of the outer membrane is estimated to be about 100Å from the $A_0(u)$ (Ueki *et al.*, 1979; Kataoka & Ueki, 1980). These results about chromatophore and the outer membrane suggest that the indexing of intensity maxima sometimes led to erroneous conclusions as for the arrangement of molecules in an assembly with finite size (also see APPENDIX). In such scattering systems, the radial autocorrelation function, $A_0(u)$, provides useful information about the structure of the scatterer.

(b) Effect of Background Subtraction on $A_0(u)$.

Although $A_0(u)$ is directly derived from the observed intensity function without any assumption, there are two problems encountered in the analysis of such a system: one is the background subtraction to obtain an intensity function from the experimental data and the other is the truncation effect.

The background scattering mainly arises from proteins, lipids and other molecules that are not incorporated in the highly organized structure of protein assembly, as well as the scattering from solvent, incoherent scattering and parasitic scattering from X-ray optics. The background scattering can be estimated experimentally by the measurement of solvent, or by the scattering curve of the meridional direction, but certain ambiguity remains in most cases.

The effects of background subtraction on $A_0(u)$ were examined by using intensity data from chromatophore. In Fig. II-3, equatorial intensity data of chromatophore and various background were depicted. Background 1 is so estimated that intensities at minima in diffraction profile become zero. Background 2 is the one used to calculate the $A_0(u)$ shown in Fig. II-2 (see EXPERIMENTAL PROCEDURES). Background 3 is estimated by measuring optical density along 45° to the equator and multiplying appropriate factor. This background is contaminated with

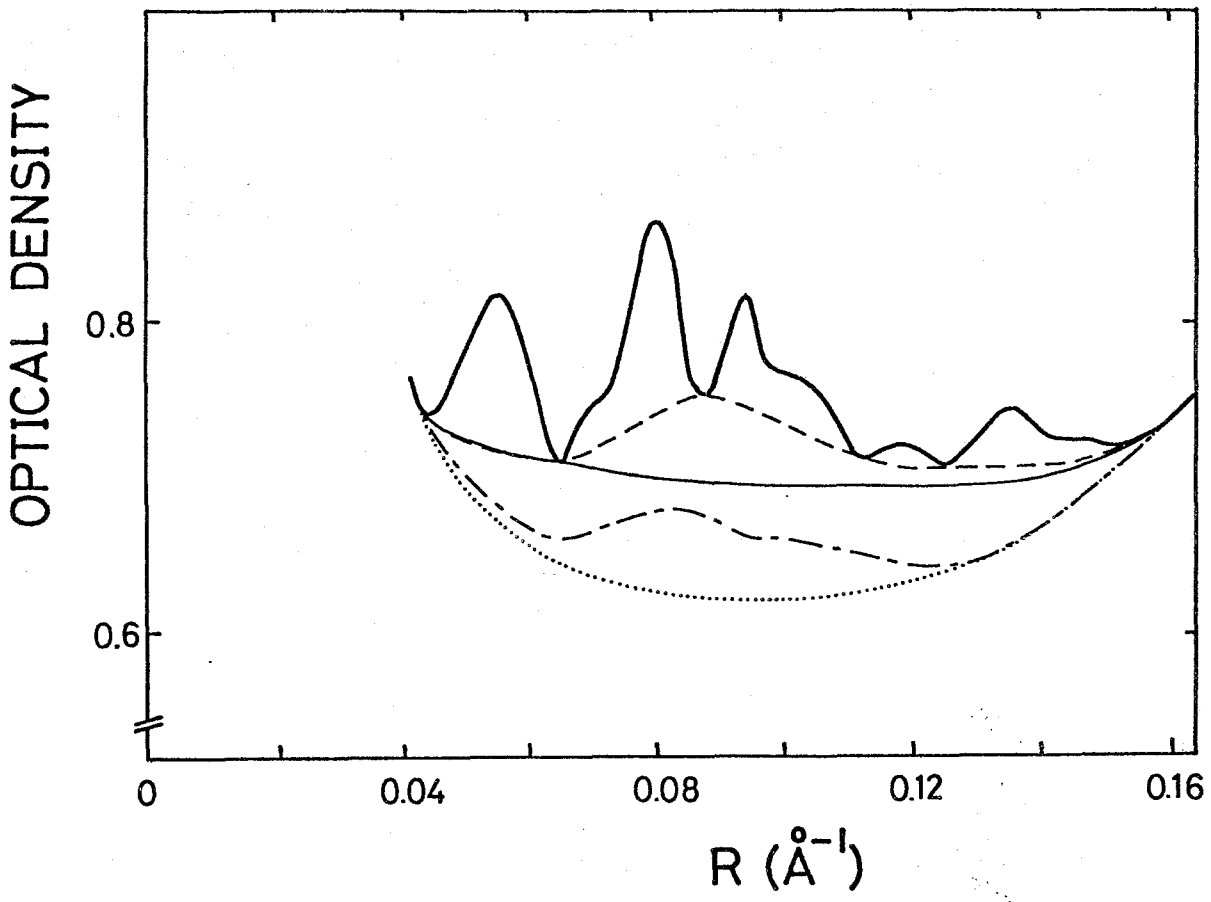

Fig. II-3. Intensity data and various estimated background scatterings. -----: background 1; ———: background 2; -•-•-: background 3 and •••••: background 4. See text for estimation of each background.

both the equatorial and the meridional reflections. Background 4 is estimated from the scattering from the buffer solution. Intensity functions, $I_0(R)$'s, were obtained by subtracting each background and were transformed into $A_0(u)$'s. Each $A_0(u)$ is expressed in Fig. II-4. Each $A_0(u)$ is identical in the region, $u \geqq 40\text{Å}$. In the region, $u \leqq 40\text{Å}$, peak positions of vector magnitudes in $A_0(u)$ are a little shifted each other (shifts are within 2Å), and peak heights change considerably, especially, the peak height of $u \simeq 10\text{Å}$.

In the approach of the radial autocorrelation function presented in this chapter, we utilized peak positions and were not concerned with the quantitative analysis of heights of peaks. Therefore, the proper estimation of background level is enough to give the reasonable results.

As for the truncation effect, peak positions in $A_0(u)$ is little influenced, except for small u region, as a result of calculations of the model structures. Thus, the above discussion is also valid if $A_0(u)$ is calculated through $I_0(R)$ at the resolution of about 7Å.

(c) Interpretation of $A_0(u)$ of Chromatophore by $a_n(u)$.

From the ratios of peak positions of $A_0(u)$, the structure with six-fold rotational axis is deduced for the structure of the photosynthetic unit. The $A_0(u)$ shown in Fig. II-2 was calculated from $I_0(R)$ in the range of

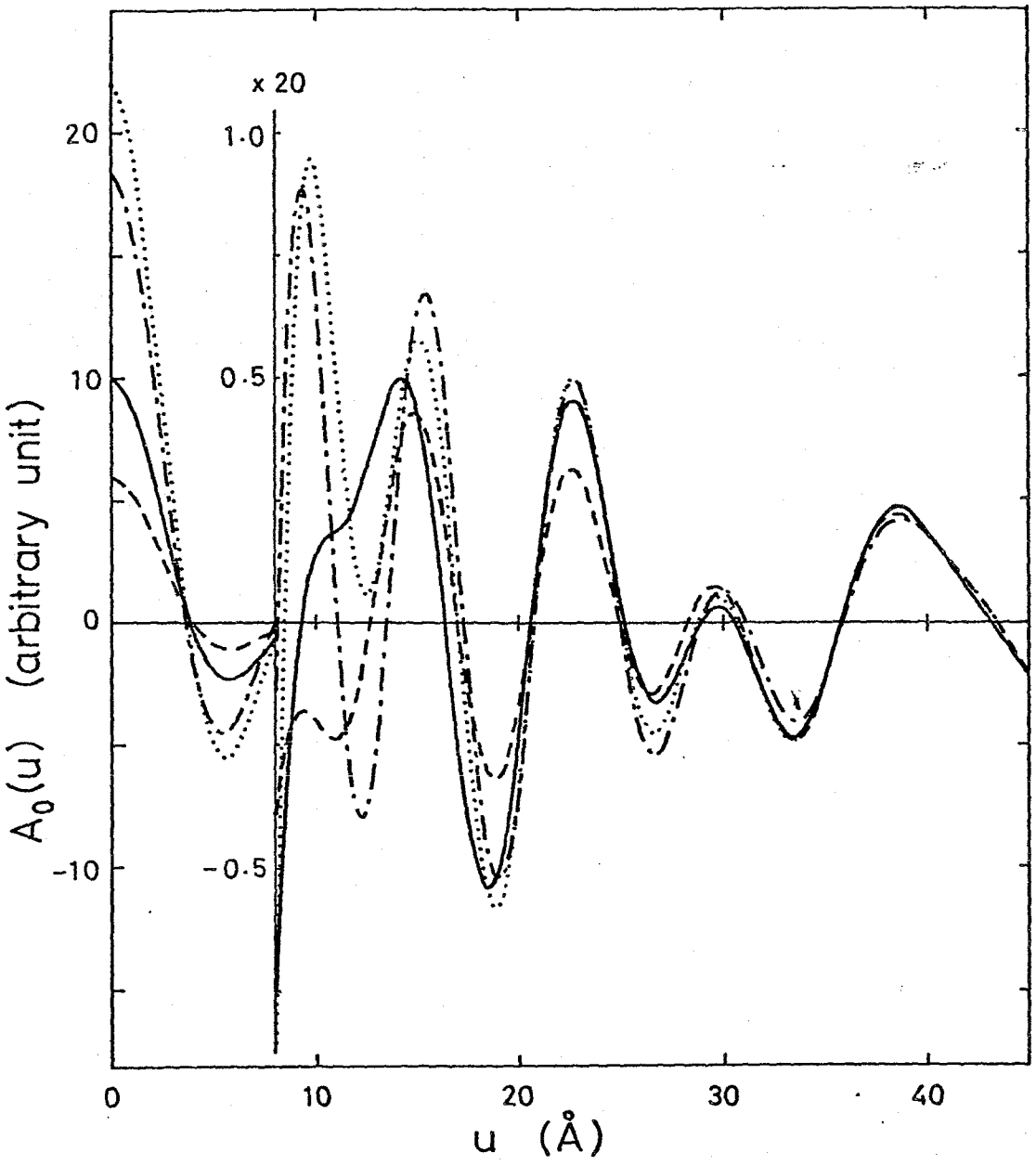

Fig. II-4. Radial autocorrelation functions calculated from intensity functions with different background subtraction. Each line is calculated from the intensity function subtracting the background expressed by the same line in Fig. II-3. Each function is normalized to the value at origin of the function indicated by solid line which is the same function as shown in Fig. II-2. The value at origin of each function corresponds to the integral value of each intensity function.

$0.04\text{Å}^{-1} \leqq R \leqq 0.16\text{Å}^{-1}$. We did not use the $I_0(R)$ in small-angle region, since we could not obtain decisive diffraction pattern in this region. This means that $I_0(R)$ approximately lacks the term $|F_0(R)|^2$ and hence $A_0(u)$ contains the terms $a_n(u)$'s with $n \neq 0$. As was indicated in the former section, minima of $[A_0(u) - a_0(u)]$ are meaningful and may give useful clues for $a_n(u)$. In Table II-3 ∿ 6, the estimation of $a_n(u)$ are tried by comparing of the ratios between maxima and minima. By assuming n = 2, 3, 4 or 6, a great part of maxima and minima are explained. Consequently, four plausible symmetry elements, two-, three-, four- and six-fold rotational symmetry are the conceivable symmetry elements of the photosynthetic unit. Thus, we have again the possibility that the structure of the photosynthetic unit is the one with rotational symmetry. At present stage, we have no other experimental evidence to conclude the symmetry element.

(d) Comparison with the Result Obtained by Electron Microscopy.

Recently, Miller (1979) reported the structural study of thylakoid membrane of *Rhodopseudomonas viridis* by electron microscopy (Fig. II-5). He revealed that the membranes are composed of a sheet of apparently identical subunits arranged in a hexagonal fashion, and that the individual subunits repeat at a distance of 110Å.

TABLE II-3

INTERPRETATION OF MAXIMA AND MINIMA, u_i, OF $A_0(u)$ BY $a_2(u)$.

expected maximum: u_0.

expected minimum: $0.707u_0$.

u_i (Å) \ u_0 (Å)	EXPECTED MAXIMA OR MINIMA (Å)					
	110.0	102.5	97.5	66.5	61.3	38.5
10.5						
12.5						
14.5						
18.7						
22.8						
26.8						*27.2*
30.0						
33.5						
38.5						38.5
41.0					*43.3*	
43.5						
47.3				*47.0*		
52.5						
57.3						
61.3					61.3	
63.0						
66.5				66.5		
71.0		*72.5*	*68.9*			
76.0						
80.0	*77.8*					
87.5						
93.0						
97.5			97.5			
100.0						
102.5		102.5				
106.0						
110.0	110.0					
113.5						
118.0						

Italic numbers indicate minima.

TABLE II-4

INTERPRETATION OF MAXIMA AND MINIMA, u_i, OF $A_0(u)$ BY $a_3(u)$

expected maximum: $0.866u_0$.

expected minima: $0.5u_0$, u_0.

u_i (Å) \ u_0 (Å)	EXPECTED MAXIMA OR MINIMA (Å)					
	113.5	*100.0*	*80.0*	*71.0*	*63.0*	*57.3*
10.5						
12.5						
14.5						
18.7						
22.8						
26.8						*28.7*
30.0						
33.5				*35.5*	*31.5*	
38.5						
41.0			*40.0*			
43.5						
47.3		*50.0*				
52.5					54.6	49.6
57.3	*56.8*					*57.3*
61.3				61.5		
63.0					*63.0*	
66.5			69.2			
71.0				*71.0*		
76.0						
80.0			*80.0*			
87.5		86.6				
93.0						
97.5	98.3					
100.0		*100.0*				
102.5						
106.0						
110.0						
113.5	*113.5*					
118.0						

Italic numbers indicate minima.

TABLE II-5

INTERPRETATION OF MAXIMA AND MINIMA, u_i, OF $A_0(u)$ BY $a_4(u)$.

expected maxima: $0.707u_0$, u_0.

expected minima: $0.383u_0$, $0.924u_0$.

u_i (Å) \ u_0 (Å)	EXPECTED MAXIMA OR MINIMA (Å)							
	110.0	102.5	97.5	87.5	76.0	61.3	52.5	43.5
10.5								
12.5								
14.5								
18.7							*20.1*	*16.7*
22.8								
26.8					*29.1*	*23.5*		
30.0								30.7
33.5			*37.3*	*33.5*				
38.5							37.1	
41.0	*42.1*	*39.3*						*40.1*
43.5						43.3		43.5
47.3							*48.5*	
52.5					53.7		52.5	
57.3						*56.6*		
61.3				61.9		61.3		
63.0								
66.5			68.9					
71.0					*70.2*			
76.0	77.8	72.5			76.0			
80.0				*80.9*				
87.5				87.5				
93.0		*94.7*	*90.0*					
97.5			97.5					
100.0	*101.6*							
102.5		102.5						
106.0								
110.0	110.0							
113.5								
118.0								

Italic numbers indicate minima.

TABLE II-6

INTERPRETATION OF MAXIMA AND MINIMA, u_i, OF $A_0(u)$ BY $a_6(u)$.

expected maxima: $0.5u_0$, $0.866u_0$, u_0.

expected minima: $0.259u_0$, $0.707u_0$, $0.966u_0$.

u_i (Å) \ u_0 (Å)	EXPECTED MAXIMA OR MINIMA (Å)							
	118.0	110.0	102.5	97.5	87.5	76.0	66.5	61.3
10.5								
12.5								
14.5								
18.7					*22.7*	*19.7*	*17.2*	*15.8*
22.8								
26.8		*28.5*	*26.5*	*25.3*				
30.0							33.2	30.7
33.5	*30.6*							
38.5						38.0		
41.0								*43.3*
43.5					43.8			
47.3							*47.0*	
52.5		55.0	51.3	48.8				53.1
57.3						*53.7*		*59.2*
61.3	59.0						57.6	61.3
63.0					*61.9*		*64.2*	
66.5						65.8	66.5	
71.0			*72.5*	*68.9*		*73.4*		
76.0					75.7	76.0		
80.0	*83.4*	*77.8*			*84.5*			
87.5			88.8	84.4	87.5			
93.0				*94.2*				
97.5		95.3		97.5				
100.0			*99.0*					
102.5	102.2		102.5					
106.0		*106.3*						
110.0		110.0						
113.5	*114.0*							
118.0	118.0							

Italic numbers indicate minima.

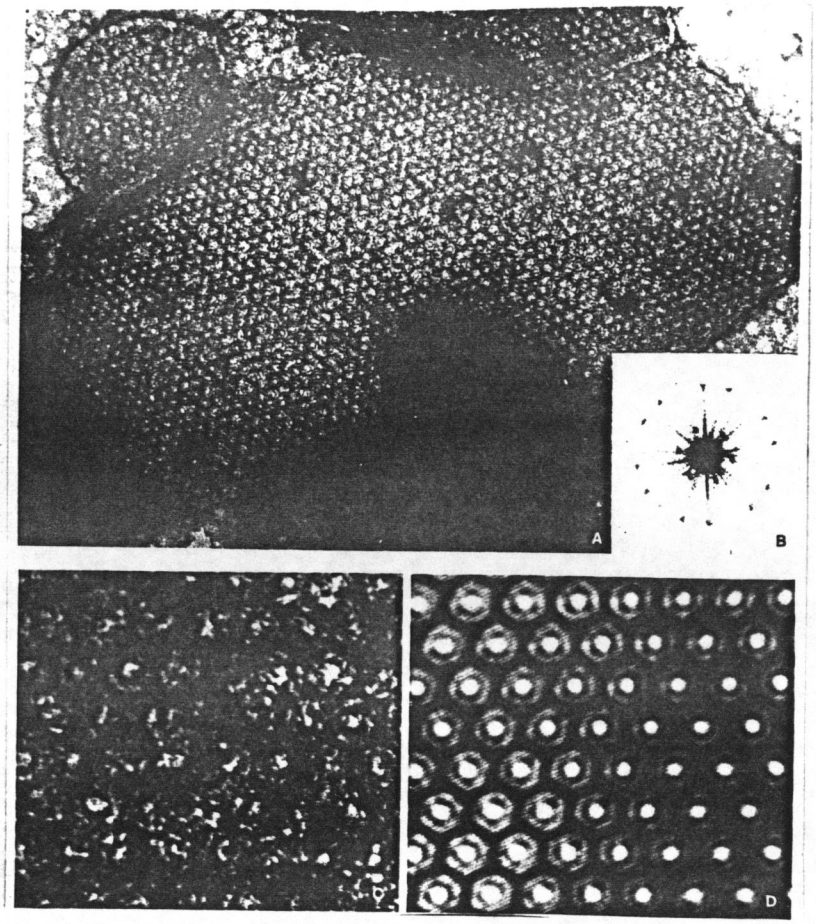

Fig. II-5. Electron microscopic study of thylakoid membrane of *Rps. viridis*. (a) Negatively stained electron micrograph of thylakoid membrane, (b) optical transform of the micrograph in (a), (c) Higher magnification view of the negatively stained membrane shown in (a), and (d) digitally filtered image obtained from (c) with the use of the transform (b). (Miller, 1979)

By filtering technique, details of each subunit were also obtained. According to it, each subunit has six-fold rotational symmetry. (Our visual examination for Fig. II-5 seems to lead the conclusion of three-fold rotational symmetry rather than six-fold one.) However, he did not refer to the function of the particle.

We have not examined *Rps. viridis* by X-ray diffraction. However, our X-ray experiments suggest that all photosynthetic bacteria have highly organized structures in their photosynthetic apparatus and they are probably photosynthetic units (Inai, 1980; Inai *et al.*, 1980). Moreover, even though diffraction patterns of chromatophores from purple non-sulfur bacteria are different from each other, their radial autocorrelation functions give the same peak positions, indicating that the internal structures of them resemble quite well to each other (Inai, 1980; Inai *et al.*, 1980). *Rps. viridis* is a kind of purple non-sulfur bacteria, as well as *R. rubrum*. Therefore, we conclude that the particle visible in electron micrograph (Fig. II-5) is a photosynthetic unit, and the structure is not far different from the structure of *R. rubrum* photosynthetic unit.

In Table II-7, the results obtained by X-ray diffraction (our results) are compared with those obtained by electron microscopy. In the Table, we can see the complementation of both techniques in the structure study.

TABLE II-7

COMPARISON OF THE "PARTICLE" STRUCTURE
VISIBLE BY
X-RAY DIFFRACTION AND ELECTRON MICROSCOPY

	X-ray diffraction	Electron microscopy
Bacterial species	*Rhodospirillum rubrum*	*Rhodopseudomonas viridis*
Identity of "particle"	Photosynthetic unit	unknown (maybe photosynthetic unit)
Maximum dimension	110 ∿ 130Å	110Å
Symmetry element	Rotational symmetry (2, 3, 4, or 6-fold)	6-fold rotational symmetry (3-fold ?)
Distribution of "particle"	random	two-dimensional hexagonal fashion
Internal fine structure	Existence of electron density fluctuations in the electron density projection is predicted.	Low electron density region and high electron density region are visible.

X-ray diffraction is superior to electron microscopy in the identification of "particle", *i. e.*, the investigation in native state. Because of difficulties of the analysis of X-ray diffraction pattern, the former is inferior to the latter in the intuitive understanding of morphological image.

The lattice structure of the *Rps. viridis* thylakoid seems to be unique among photosynthetic bacteria (Drews, 1978). Except for this point, both results are in fair agreements with each other. Our interpretation by means of radial autocorrelation function, therefore, is supported by electron microscopy.

II-6. SUMMARY

Results obtained by the studies described in this chapter may be summarized as follows.

(1) The photosynthetic unit is not a microcrystal, even if the equatorial reflection can be indexed as a two-dimensional hexagonal lattice with a = 42.6Å.

(2) The approximate size of the photosynthetic unit is about 110 ∿ 130Å.

(3) The arrangement of the units in the chromatophore membrane is random.

(4) Protein molecules in the unit form a rigid structure, being arranged mutually in the fixed positions to give distinct X-ray diffraction pattern.

(5) The most probable structure is the one which possesses a rotational symmetry.

(6) Radial autocorrelation function which is calculated directly from the X-ray intensity data is effective to interpret the diffuse but distinct X-ray diffraction pattern such as that of chromatophore.

APPENDIX

Estimation of $A_0(u)$ for Arrangement of Bacteriorhodopsin in Purple Membrane.

The structure of the purple membrane was established by the filtering technique of electron micrographs (Unwin & Henderson, 1975). The essence of the structure is a two-dimensional hexagonal arrangement of trimers of protein, bacteriorhodopsin, with cell edge 62.7Å. The trimer has a three-fold rotational symmetry (Fig. II-6). The monomer is composed of seven rod-like structures. The rods were found to be the α-helices by X-ray diffraction (Henderson, 1975; Blaurock, 1975), and are approximately parallel to each other, being parallel to the z axis.

Circular symmetrical intensity functions were calculated for the monomer and trimer by using the formula given in the paper by Oster and Riley (1952):

$$I_0(R) = f^2(R) \sum_i \sum_j J_0(2\pi r_{ij} R)$$

where r_{ij} is a vector magnitude between α-helices, and $f(R)$ is the Fourier transform of electron density distribution, $\rho(r)$, of α-helix which is assumed by a circular symmetric Gaussian function,

$$\rho(r) = \exp[-(1/2)(r/\Delta r)^2]$$

where Δr = 2.17Å. Figure II-7 shows intensity functions

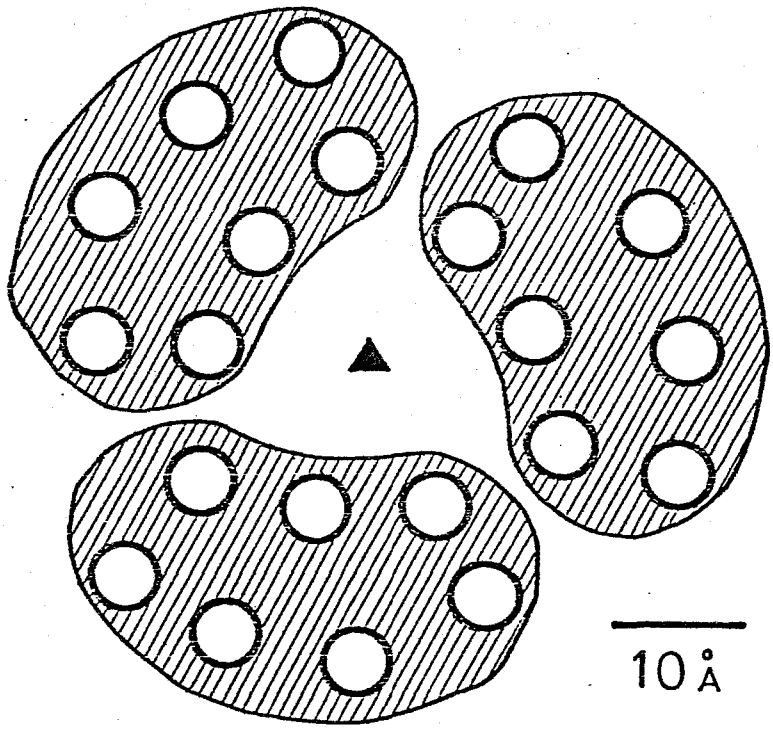

Fig. II-6. Model structure of the trimer of bacteriorhodopsin projected along z axis. The shaded regions show the monomers of bacteriorhodopsin which are arranged about a three-fold rotational axis to form a trimer. The open circles show the seven α-helices (rods) which are parallel to each other. Rods have high electron density in the structure. When trimers are arranged according to a two-dimensional hexagonal lattice with a = 62.7Å, the structure of the purple membrane is formed. The original structure was presented by Unwin and Henderson (1975).

for monomer, trimer of bacteriorhodopsin molecules and the intensity for purple membrane which was taken from the paper by Henderson (1975). The monomer gives a continuous intensity function which has only one broad diffraction maximum at $d \simeq 10\text{Å}$. The trimer apparently causes fine structure in the intensity profile. The broken line in Fig. II-7 has similar features to the observed intensity from chromatophore: broad but distinct diffraction maxima. Therefore, we can conclude that such a regular arrangement provides small- and moderate-angle diffraction patterns up to a spacing of $6 \sim 7\text{Å}$. Five maxima in the diffraction profile from trimer can be indexed as a two-dimensional hexagonal lattice with $a = 80\text{Å}$. This indexing is, of course, not meaningful, since the rods in the trimer have no crystalline arrangement as is clear from Fig. II-6. This fact indicates that indexing of a diffraction pattern may sometimes lead to incorrect conclusions for the X-ray scatterers with such profiles. The intenisty function for purple membrane consists of sharp Bragg reflections; they can be indexed as a two-dimensional hexagonal lattice with $a = 62.7\text{Å}$ (Blaurock & Stoeckenius, 1971).

Radial autocorrelation functions calculated from the intensities in Fig. II-7 are shown in Fig. II-8. They correspond to the structures of monomer, trimer and purple membrane as below.

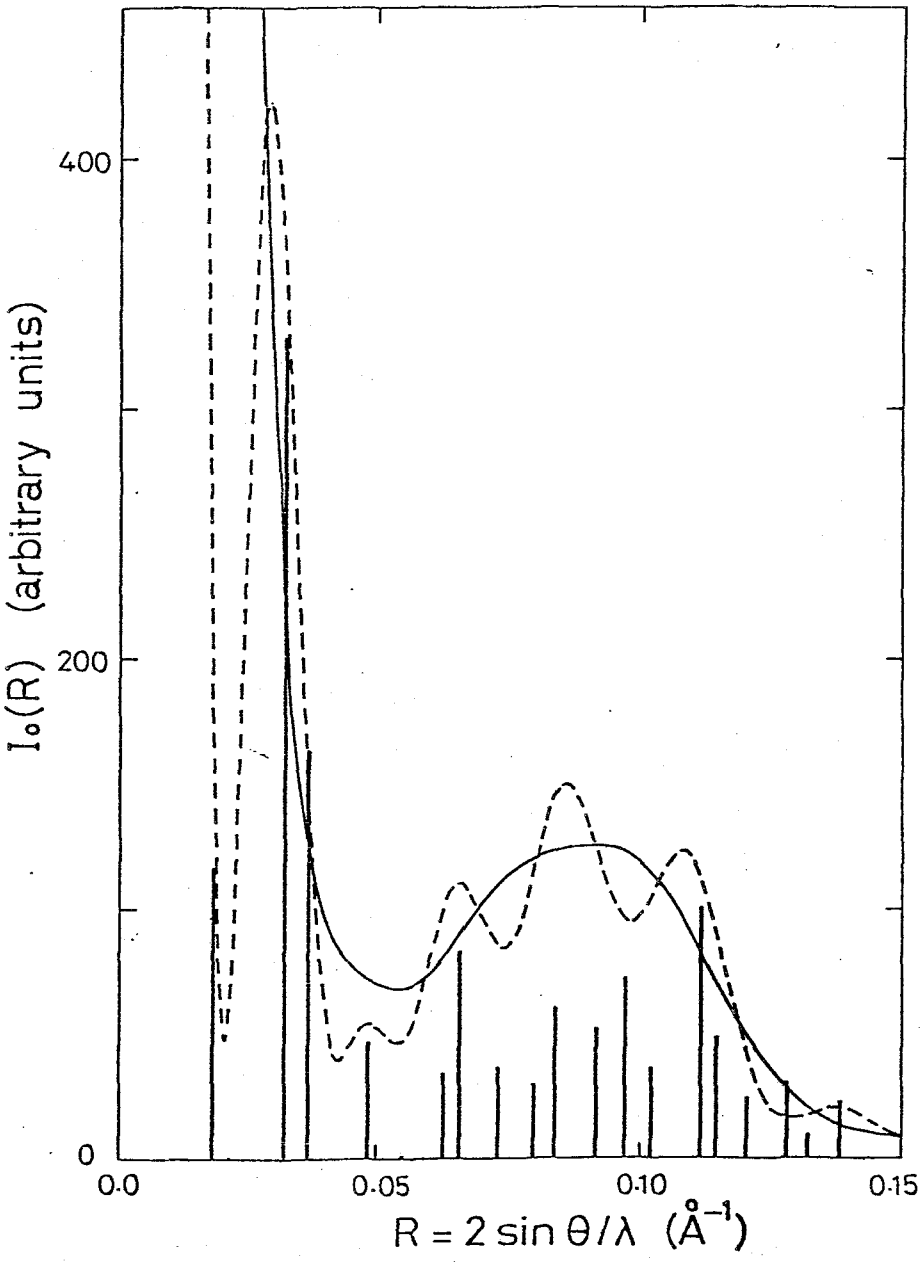

Fig. II-7. Equatorial intensity functions, $I_0(R)$, for monomer and trimer of bacteriorhodopsin and purple membrane. Solid line: monomer, broken line: trimer and vertical lines: Bragg reflections of purple membrane (taken from Henderson (1975)).

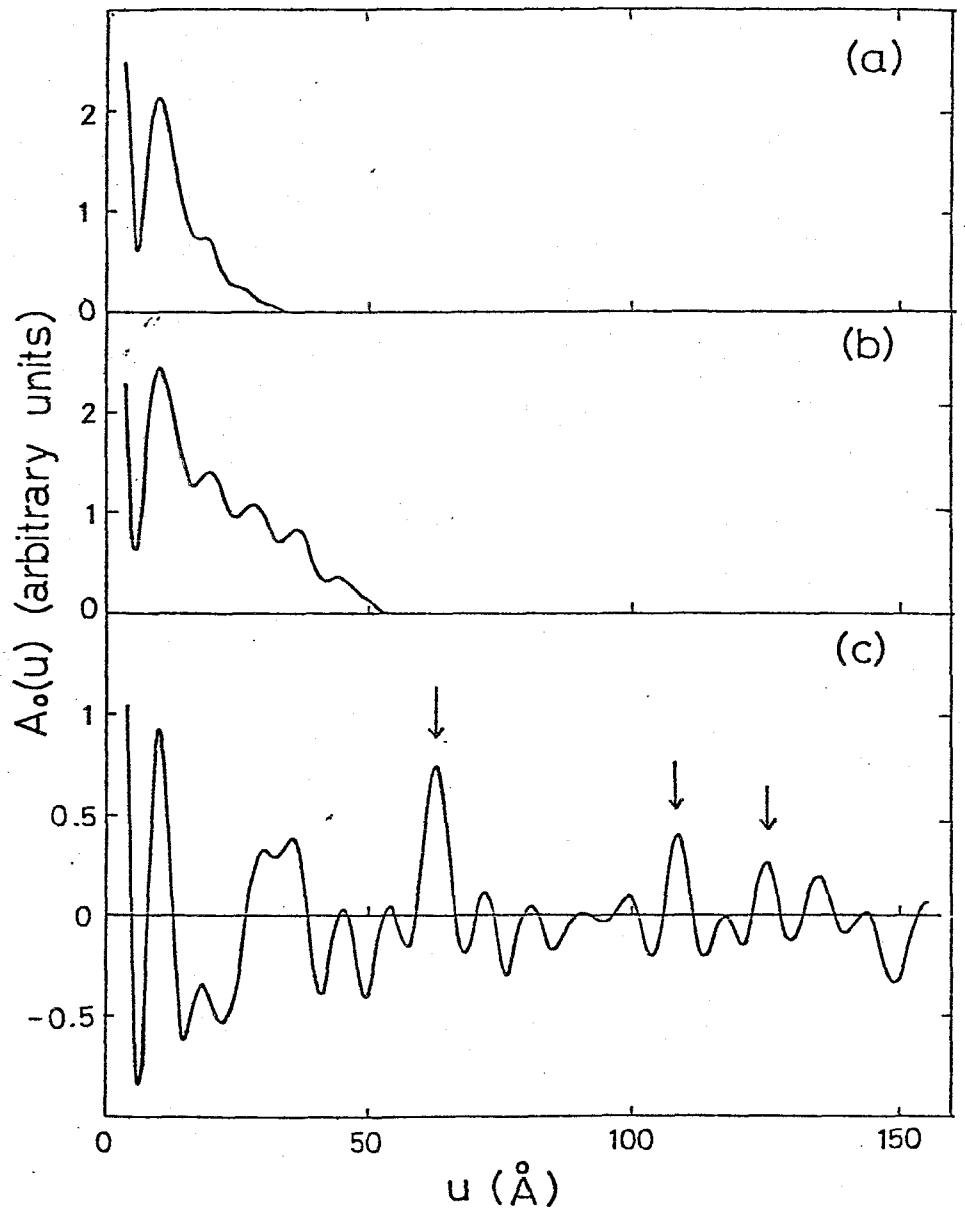

Fig. II-8. Radial autocorrelation functions, $A_0(u)$, for (a) monomer, (b) trimer of bacteriorhodopsin and (c) purple membrane. Arrows in (c) indicate the expected positions of vectors from the two-dimensional hexagonal arrangement of trimers.

(i) $A_0(u)$'s for monomer and trimer decreases to zero at about 33Å and 53Å, in agreement with sizes of the scatterers, while that for the purple membrane does not.

(ii) $A_0(u)$ for the purple membrane gives evidently the peaks due to the two-dimensional hexagonal arrangement of trimers, at u = 63Å, 109Å, 126Å, and so on which correspond to the first, second, third ... neighbours in the lattice. In addition, there are peaks which come from the intra-trimer vectors. On the other hand, $A_0(u)$ for the trimer does not have peaks at u = 80Å and so on which must appear if the above-mentioned hexagonal lattice (a = 80Å) is correct. Therefore, the indexing of the diffraction profile for the trimer is only by accident.

(iii) Fine structures of the former two can be interpreted on the basis of inter-rod distances (see Fig. II-6). Peaks in $A_0(u)$ for the monomer reflect the intra-molecular structure of the bacteriorhodopsin molecule, *i. e.*, a peak at about 10Å in $A_0(u)$ is from the nearest neighbour distances of rods. The fact that no other appreciable peaks are observed in $A_0(u)$ for the monomer implies that there is no regular arrangement of rods in a molecule. $A_0(u)$ for the trimer gives information as to the intra- and inter-molecular vectors. It gives more distinct peaks due to the

regular arrangement of rods in the trimer according to three-fold rotational symmetry; the contribution of terms $a_n(u)$'s to $A_0(u)$ in addition to $a_0(u)$ is very appreciable, especially $a_3(u)$ and higher terms.

CHAPTER III

STRUCTURE OF CHROMATOPHORE

STRUCTURE OF CHROMATOPHORE

On the basis of the results obtained in both chapters, the outline of a chromatophore is depicted in Fig. III-1 schematically. The diameter of a vesicle, 600Å, was given by electron microscopy (Oda & Horio, 1964). The X-ray scatterer expressed by solid ellipse in the figure is the photosynthetic unit. The unit is composed of the main body (photoreaction unit) and the loosely bound components (oxidation-reduction components such as ubiquinone-10 protein and cytochrome c_2) (Fig. III-2). All bacteriochlorophylls are included in photosynthetic units. The region occupied by lipids are expected to cover a wide area of the membrane. There are, on the average, 24 photosynthetic units in a chromatophore (Nishi *et al.*, 1979), and no spatial correlation exists between the units. The photosynthetic unit has well-defined internal structure, and the structure is deduced to be the one with rotational symmetry.

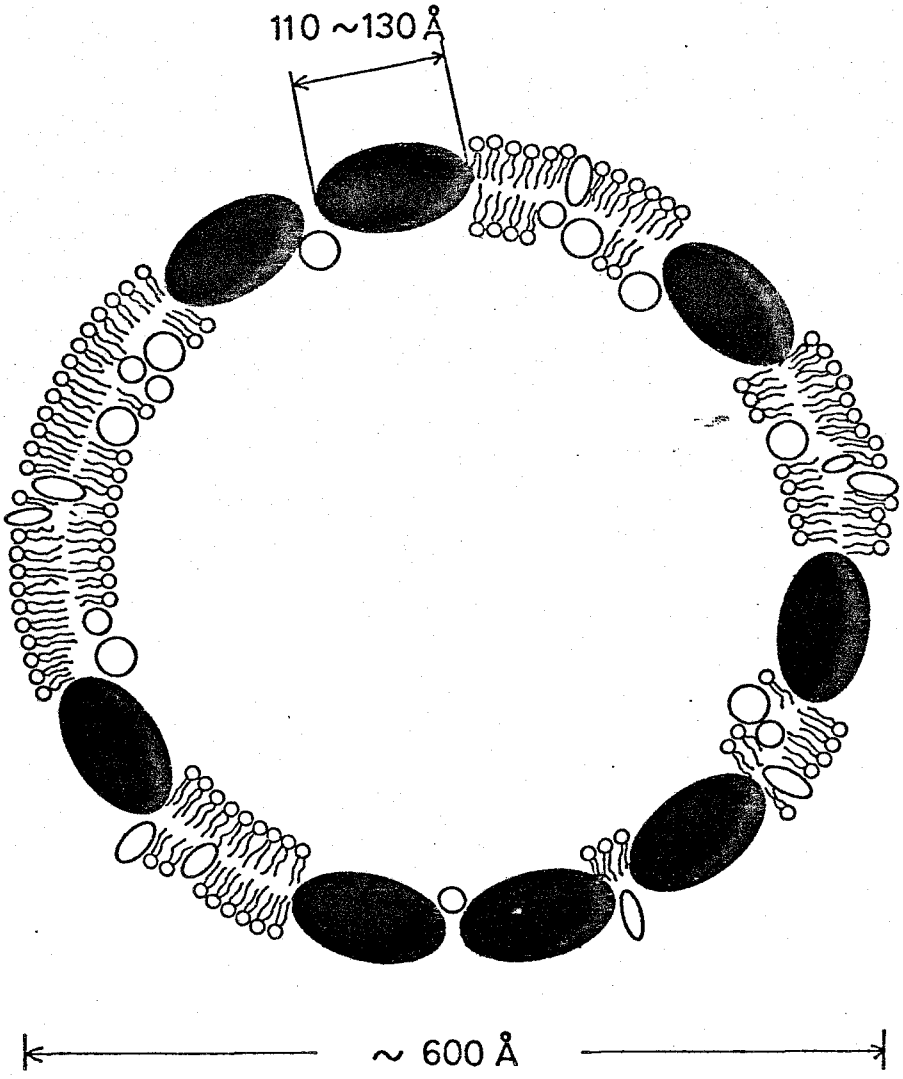

Fig. III-1. Schematic picture of a chromatophore. X-ray scatterer ( ) is photosynthetic unit which is composed of photoreaction unit, oxidation-reduction components and other few molecules (see Fig. III-2). As is seen in the picture, X-ray scatterers are randomly distributed in the chromatophore membrane. Proteins and other components which are not incorporated into the X-ray scatterer are also depicted (, , ,), although information about the locations of these components are still lacking.

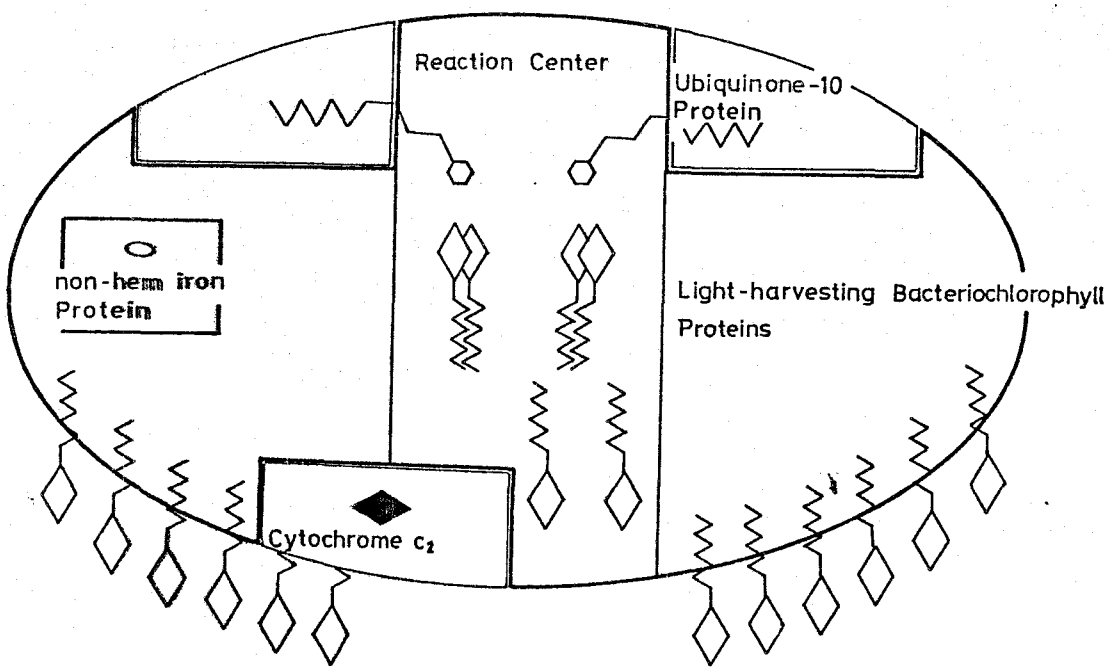

Fig. III-2. Components of the X-ray scatterer of chromatophore. The part depicted by thick solid line is the tight basic structure of the scatterer, photoreaction unit, and loosely bound components, ubiquinone-10 protein and cytochrome c_2, are expressed by thin line. ◇〰: bacteriochlorophyll; ⬡〰 : ubiquinone-10, ◆ : heme; ○ : non-heme iron, respectively.

LIST OF PUBLICATIONS

The present thesis is based on the contribution of the author to the following papers which have been published or will be published.

1. Structural Order in Chromatophore Membranes of *Rhodospirillum rubrum*.

   T. Ueki, M. Kataoka, & T. Mitsui,
   Nature, 262, 809-810, (1976)

2. Disintegration of *Rhodospirillum rubrum* Chromatophore Membrane into Photoreaction Units, Reaction Centers, and Ubiquinone-10 Protein with Mixture of Cholate and Deoxycholate.

   N. Nishi, M. Kataoka, G. Soe, T. Kakuno, T. Ueki, J. Yamashita, & T. Horio,
   Journal of Biochemistry, 86, 1211-1224, (1979)

3. The Significance of the Radial Autocorrelation Function for the Interpretation of Equatorial Diffraction from Biological Membranes.

   M. Kataoka, & T. Ueki,
   Acta Crystallographica, A36, 282-287, (1980)

4. X-ray Diffraction Studies on Chromatophore Membrane from Photosynthetic Bacteria. I. Diffraction Pattern of Photoreaction Unit Isolated from *Rhodospirillum rubrum* Chromatophore and Characteristics of Structure.

   M. Kataoka, & T. Ueki,
   submitted for publication to *Journal of Biochemistry*.

REFERENCES

Arndt, U. W. & Riley, D. P. (1952). *Proc. Roy. Soc.* 247, 409-439.

Arntzen, C. J. & Briantais, J.-M. (1975). In *Bioenergetics of Photosynthesis* (Govindjee ed.) pp. 51-113, Academic Press, New York.

Benson, A. A. (1966). *J. Amer. Oil Chemist Soc.* 43, 265-270.

Blaurock, A. E. (1975). *J. Mol. Biol.* 93, 139-158.

Blaurock, A. E. & Stoeckenius, W. (1971). *Nature New Biol.* 233, 152-155.

Buerger, M. J. (1951). *Vector Space and its Application in Crystal-Structure Investigation*, John Wiley, New York.

Casper, D. L. D., Goodenough, D. A., Makowski, L. & Phillips, W. C. (1977). *J. Cell Biol.* 74, 605-628.

Clayton, R. K. & Haselkorn, R. (1972). *J. Mol. Biol.* 68, 97-105.

Clayton, R. K. & Yamamoto, T. (1976). *Photochem. Photobiol.* 24, 67-70.

Cuendet, R. A., Zürrer, H., Snozzi, M. & Zuber, H. (1978). *FEBS Lett.* 88, 309-312.

Drews, G. (1978). *Curr. Top. Bioenerget.* 8, 161-207.

Dupont, Y., Cohen, J. B. & Changeux, J.-P. (1974). *FEBS Lett.* 40, 130-133.

Earnshaw, W., Casjens, S. & Harrison, S. C. (1976). *J. Mol. Biol.* 104, 387-410.

Elliott, A. (1965). *J. Sci. Instrum.* 42, 312-316.

Emerson, R. & Arnold, W. (1932). *J. Gen. Physiol.* 15, 391-420.

Feick, R. & Drews, G. (1978). *Biochim. Biophys. Acta* 501, 499-513.

Franklin, R. E. & Klug, A. (1955). *Acta Cryst.* 8, 777-780.

Giesbrecht, P. & Drews, G. (1966). *Arch. Mikrobiol.* 54, 297-330.

Govindjee & Govindjee, R. (1975). In *Bioenergetics of Photosynthesis* (Govindjee ed.) pp. 1-50, Academic Press, New York.

Haverkate, F., Teulings, F. A. G. & van Deenen, L. L. M. (1965). *Koninkl. Ned. Akad. Wetenschap. Proc.* B68, 154-159.

Henderson, R. (1975). *J. Mol. Biol.* 93, 123-138.

Hiraki, K., Hamanaka, T., Mitsui, T. & Kito, Y. (1978). *Biochim. Biophys. Acta* 536, 318-322.

Holt, S. C. & Marr, A. G. (1965). *J. Bacteriol.* 89, 1413-1420.

Horio, T. & Kamen, M. D. (1961). *Biochim. Biophys. Acta* 48, 266-286.

Horio, T., Nishikawa, K., Katsumata, M. & Yamashita, J. (1965). *Biochim. Biophys. Acta* 94, 371-382.

Huzisige, H. (1973). *Kogosei (Photosynthesis)* (in Japanese), Shokabo, Tokyo.

Huzisige, H., Usiyama, H., Kikuti, T. & Azi, T. (1969). *Plant & Cell Physiol.* 10, 441-455.

Inai, K. (1980). Master Thesis, Faculty of Engineering Science, Osaka University.

Inai, K., Kataoka, M. & Ueki, T. (1980). manuscript in preparation.

Kakuno, T., Bartsch, R. G., Nishikawa, K. & Horio, T. (1971). *J. Biochem. (Tokyo)* 70, 79-94.

Kamen, M. D. (1963). *Primary Processes in Photosynthesis*, Academic Press, New York.

Kataoka, M. (1976). Master Thesis, Faculty of Engineering Science, Osaka University.

Kataoka, M. & Ueki, T. (1980). *Acta Cryst.* A36, 282-287.

Kok, B. (1956). *Biochim. Biophys. Acta* 21, 245-258.

Kreutz, W. (1963a). *Z. Naturf.* 18b, 567-571.

Kreutz, W. (1963b). *ibid.* 18b, 1098-1104.

Kreutz, W. (1964). *ibid.* 19b, 441-446.

Kreutz, W. (1965). *Nature* 206, 1358-1359.

Kreutz, W. & Menke, W. (1960a). *Z. Naturf.* 15b, 402-410.

Kreutz, W. & Menke, W. (1960b). *ibid.* 15b, 483-487.

Kreutz, W. & Menke, W. (1962). *ibid.* 17b, 675-683.

Kreutz, W. & Weber, P. (1966). *Naturwissenschaften* 53, 11-14.

Laemmli, U. K. (1970). *Nature* 227, 680-685.

Langridge, R., Barron, P. D. & Sistrom. W. R. (1964). *Nature* 204, 97-98.

Lommen, M. A. J. & Takemoto, J. (1978). *J. Bacteriol.* 136, 730-741.

MacGillavry, C. H. & Bruins, E. M. (1948). *Acta Cryst.* 1, 156-158.

Mannella, C. A. & Bonner, W. D. Jr. (1975). *Biochim. Biophys. Acta* 413, 226-233.

Matsuda, H., Kakuno, T. & Horio, T. (1980). personal communication; to be published.

Menke, W. (1960). *Z. Naturf.* 15b, 479-482.

Miller, K. R. (1979). *Proc. Natl. Acad. Sci. USA* 76, 6415-6419.

Miller, K. R., Miller, G. J. & McIntyre, K. R. (1976). *J. Cell Biol.* 71, 624-638.

Moskalenko, A. A. & Erokhin, Yu. E. (1978). *FEBS Lett.* 87, 254-256.

Nishi, N., Kataoka, M., Soe, G., Kakuno, T., Ueki, T., Yamashita, J. & Horio, T. (1979). *J. Biochem (Tokyo)* 86, 1211-1224.

Nishimura, M. (1970). *Biochim. Biophys. Acta* 197, 69-77.

Nishimura, M. (1975). *Kogosei no Shokikatei (Primary Processes in Photosynthesis)* (in Japanese), Kyoritsu Shuppan, Tokyo.

Noël, H., van der Rest, M. & Gingras, G. (1973). *Biochim. Biophys. Acta* 275, 219-230.

Oda, T. & Horio, T. (1964). *Exptl. Cell Res.* 34, 414-416.

Oelze, J. & Golecki, J. R. (1975). *Arch. Microbiol.* 102, 59-64.

Ogawa, T., Obata, F. & Shibata, K. (1966). *Biochim. Biophys. Acta* 112, 223-234.

Ohki, R. & Takamiya, A. (1970). *Biochim. Biophys. Acta* 197, 240-249.

Okamura, M. Y., Steiner, L. A. & Feher, G. (1974). *Biochemistry* 13, 1394-1402.

Okayama, S., Yamamoto, N., Nishikawa, K. & Horio, T. (1968). *J. Biol. Chem.* 243, 2995-2999.

Oster, G. & Riley, D. P. (1952). *Acta Cryst.* 5, 272-276.

Pape, E. H., Menke, W., Weick, D. & Hosemann, R. (1974). *Biophys. J.* 14, 221-232.

Pardee, A. B., Schachman, H. K. & Stainer, R. Y. (1952). *Nature* 169, 282-283.

Park, R. B. & Pon N. G. (1961). *J. Mol. Biol.* 3, 1-10.

Park, R. B. & Pon N. G. (1963). *J. Mol. Biol.* 6, 105-114.

Park, R. B. & Biggins, J. (1964). *Science* 144, 1009-1011.

Parson, W. W., Clayton, R. K. & Cogdell, R. J. (1975). *Biochim. Biophys. Acta* 387, 265-278.

Porod, G. (1951). *Kolloid Z.* 124, 83-114.

Reed, D. W., Raveed, D. & Israel, H. W. (1970). *Biochim. Biophys. Acta* 223, 281-291.

Schachman, H. K., Pardee, A. B. & Stainer, R. Y. (1952). *Arch. Biochem. Biophys.* 38, 245-260.

Shioi, Y., Takamiya, K. & Nishimura, M. (1974). *J. Biochem. (Tokyo)* 76, 241-250.

Singer, S. J. & Nicolson, G. L. (1972). *Science* 175, 720-731.

Smith, J. H. C. C. & Benitez, A. (1955). In *Moderne Methode der Pflanzenanalyse* (Peach, K. & Tracey, M. V. eds), p. 142, Springer, Berlin.

Staehelin, L. A. (1975). *Biochim. Biophys. Acta* 408, 1-11.

Staehelin, L. A. (1976). *J. Cell Biol.* 71, 136-158.

Tanaka, K. (1980). Master Thesis, Faculty of Science, Osaka University.

Thomas, J. B., Blaauw, O. H. & Duysens, L. M. N. (1953). *Biochim. Biophys. Acta* 10, 230-240.

Tôyama, S. (1977). In *Kogoseikikan no Saihoseibutsugaku (Cell Biology of Photosynthetic Apparatus)* (in Japanese) (Ishida, M., Ueda, K. & Tôyama, S. eds.), pp. 138-160, Kyoritsu Shuppan, Tokyo.

Tsukamoto, Y. (1980). Master Thesis, Faculty of Engineering Science, Osaka University.

Tsukamoto, Y., Ueki, T., Kataoka, M. & Mitsui, T. (1980). manuscript in preparation.

Ueki, T., Kataoka, M. & Mitsui, T. (1976). *Nature* 262, 809-810.

Ueki, T., Mitsui, T. & Nikaido, H. (1979). *J. Biochem. (Tokyo)* 85, 173-182.

Ueki, T., Tanaka, M., Nakae, T. & Nikaido, H. (1980). submitted to *Proc. Natl. Acad. Sci. USA*.

Unwin, P. N. T. & Henderson, R. (1975). *J. Mol. Biol.* 94, 425-440.

Vainshtein, B. K. (1966). *Diffraction of X-rays by Chain Molecules*, Elsevier, Amsterdam.

van der Grinten, W. (1932). *Phys. Z.* 33, 769-770.

van Niel, C. B. (1935). *Cold Spring Harbor Symp. Quant. Biol.* 3, 138-149.

van Niel, C. B. (1941). *Adv. Enzymol.* 1, 263-328.

Waser, J. (1955). *Acta Cryst.* 8, 142-150.

Wessels, J. S. C. (1963). *Proc. Roy. Soc.* B157, 345-355.

Wright, C. A. & Clayton, R. K. (1973). *Biochim. Biophys. Acta* 333, 246-260.